Sepsis Induces Age- and Sex-Specific Chromatin Remodeling in Myeloid-derived Suppressor Cells

Angel M. Charles[1], Dijoia B. Darden[1], Christine E. Rodhouse[1], Miguel Hernandez-Rios[1], Marie-Pierre Gauthier[2], Jason O Brant[2,3], Rhonda L. Bacher[3], Clayton E. Mathews[4], Lyle L. Moldawer[1], Philip A. Efron[1], Robert Maile[1], Michael P. Kladde[2,3].

Affiliations:

1. Sepsis and Critical Illness Research Center, Department of Surgery, College of Medicine, University of Florida, Gainesville, Florida, United States.

2. Department of Biochemistry and Molecular Biology, College of Medicine, University of Florida, Gainesville, Florida, United States.

3. Department of Biostatistics, College of Public Health & Health Professions, University of Florida, Gainesville, Florida, United States

4. Department of Pathology, Immunology and Laboratory Medicine, College of Medicine, University of Florida, Gainesville, Florida, USA

Abstract

Sepsis survivors frequently develop long-term immune dysfunction, but the epigenetic mechanisms driving persistent myeloid suppression remain poorly defined. Myeloid-derived suppressor cells (MDSCs), key immunoregulatory cells that expand during sepsis, exhibit altered function influenced by host age and sex. Here, we provide the first high-resolution epigenetic map of MDSCs following sepsis using the MAPit-FENGC method, which enables simultaneous single-molecule profiling of DNA methylation and chromatin accessibility across ~100 immune-related promoters. We employed a murine model of cecal ligation and puncture (CLP) with daily chronic stress in both young and old, male and female mice, and isolated splenic MDSCs for MAPit-FENGC analysis.

Unsupervised clustering revealed nine distinct promoter classes based on chromatin state dynamics, including classes that gain accessibility after sepsis (Classes 1–4), remain persistently closed (Class 5), or undergo age-dependent repression post-sepsis (Classes 6–8). Notably, Class 1 and 3 promoters (e.g., *S100a9*, *Mmp8*) showed robust sepsis-induced nucleosome-free region (NFR) formation across all groups, with heightened accessibility in older females. Class 2 promoters such as *Nos2* and *Cxcr2* required advanced age for activation in females, while Class 4 promoters were uniquely induced in females regardless of age. Conversely, Classes 6–8, including key regulatory genes such as *Cd274*, *Il10*, and *Nfkbiz*, lost accessibility exclusively in older septic mice, despite paradoxical DNA demethylation suggesting chromatin remodeling rather than methylation governs repression in aged hosts. Single-cell RNA sequencing of MDSC subsets corroborated promoter class distinctions, linking accessibility with transcriptional activity. These findings provide a foundation for understanding how epigenetic reprogramming, indicative of innate immune training or tolerance, of MDSCs might contribute to the divergent immune outcomes observed in different sepsis survivor populations. The resolution of select sepsis-responsive epigenetic "classes" and their members suggests these could be utilized as age or sex-specific candidate biomarkers or therapeutic targets.

Introduction

Sepsis, when the host has organ insufficiency/failure in response to infection[1], affects more than 1.7 million adults in the United States, and results in the death of greater than 350,000 of these individuals [2]. In addition, sepsis is estimated to cost in excess of $38 billion per year in America alone[3]. Although acute hospital mortality has improved[4, 5] due to measures such as the Surviving Sepsis campaign[6], long-term patient outcomes remain dismal[4, 5]. Despite the significance and impact of all the former, little to no therapeutics are available for this patient population[7].

Myeloid-derived suppressor cells (MDSCs) were delineated almost two decades ago [8], and are defined as pathologically activated myeloid cells with potent immunosuppressive activity, although many still have some pro-inflammatory properties[9]. Although the leukocytes have been investigated in the cancer field for some time, research regarding MDSCs in sepsis is relatively recent[10]. MDSCs have been demonstrated to expand and remain circulating in the sepsis survivor, and are associated with poor outcomes in these patients[11, 12]. Although these sepsis-derived MDSCs meet the key functional definition of MDSCs (immunosuppressive activity against lymphocytes, etc.), data indicates that septic-MDSC are not identical to oncologic derived MDSCs, in both mice and humans[13-15]. Modification of MDSCs in the sepsis survivor represents a potential approach to improve these patient's outcomes[16] but still requires a better disease specific understanding of these cells.

In addition to the need for more disease specific precision/personalized therapeutics for sepsis, there is a need to delineate how sepsis engenders unique effects in certain cohorts, e.g. age and sex[16-25]. Work from our group and others has illustrated that both sex and age have significant effects on the sepsis response, as well as the post-infection MDSCs generated by that host[17, 18, 20-

[22]. Thus, investigating these cohorts will be key to any successful future interventions for the sepsis survivor.

Epigenetics, the study of alterations in gene expression not due to changes in the gene code, are considered a potential method of successfully modifying MDSCs in the host so that these cells will no longer be pathologic[26]. One such method of studying the epigenetics of the sepsis-induced MDSC is Methyltransferase Accessibility Protocol for Individual Templates combined with Flap-Enabled Next-Generation Capture (MAPit-FENGC), a validated method that allows for simultaneous single-molecular level analysis of methylation and accessibility at target promoter and enhancer regions[27]. Using a preclinical surgical sepsis animal model that better imitates the human condition[17, 21], we utilized MAPit to assess the epigenetic uniqueness of isolated murine splenic $Cd11b^{+}Gr1^{+}$ MDSCs in several cohorts: sepsis versus control, male versus female, and, young adult versus older adult.

Methods

Animals

Young and old female (50%) and male (50%) mice underwent our intra-abdominal sepsis model of Cecal Ligation and Puncture (CLP) followed by daily chronic stress (DCS). Approximately eight to 12 mice were used per experimental group. Mice were euthanized 7 days post CLP + DCS. Experimental mice were euthanized in compliance with predetermined IACUC Body Condition Score (BCS) criteria. A modification to this included the following: greater than or equal to 20% weight loss from baseline or from age-matched controls if the animals are still growing during the study or greater than or equal to 20% weight loss from baseline in old mice who have a BCS of

greater than 2 in the first 5 days after CLP, or greater than 40% weight loss from baseline in old mice with a BCS greater than 2 after 5 days following CLP. Based on these criteria, no mice had to be euthanized for excessive weight loss during the course of the study.

Intra-Abdominal Sepsis Model

CLP was conducted under isoflurane anesthesia we have previously described[28]. The cecum was ligated 1 cm from its tip and a 22- or 25-gauge needle was used to puncture the cecum depending on the desired experimental mortality. Buprenorphine analgesia was provided for 48 hours post surgery. Antibiotics (imipenem monohydrate; 25 mg/kg diluted in 1 mL 0.9% sodium chloride [NaCl]) were administered 2 hours post-CLP then continued for 72 hours. DCS was conducted as previously described[29]. Briefly, this involved placing mice in weighted plexiglass animal restraint holders (Kent Scientific, Torrington, CT) for 2 hours daily starting the day after CLP. The purpose was to simulate the ICU environment, where patients are often bedbound with limited mobility. MDSC were isolated using a CD11b+Gr1+ isolation (EasySep™ Mouse MDSC (CD11b+Gr1+) Isolation Kit, StemCell, Cambridge, MA, USA) according to manufacturer's instructions and as we have described previously[21].

Single-cell RNA sequencing (scRNA-seq) analysis

Splenocytes from naive, BCG-vaccinated, septic, and BCG plus sepsis (eighteen hours post-CS) neonatal mice, were obtained after mechanical dissociation using 70 μm strainers. After centrifugation at 300 × *g* for 10 min, red blood cells (RBC) were lysed with ACK lysing buffer (Thermo Fisher Scientific, Waltham, MA) for five minutes at room temperature. Total splenocytes were washed in PBS supplemented with 2% FBS, quantified (Cellometer Auto 2000 Cell Viability

Counter; Nexcelom Bioscience, Lawrence, MA) and diluted to 10^6 cells/ml before single-cell library preparation. Libraries were prepared with Chromium Next GEM Single Cell 5' v2 kit targeting 10,000 cells/lane on the 10 × Chromium microfluidics device (10 × Genomics, Pleasanton, CA). Libraries were sequenced at a minimum depth of 20,000 read pairs per cell on an Illumina Novaseq™X plus platform (Illumina, San Diego, CA). Cell Ranger Single-Cell Software v 7.0.1 (10 × Genomics) was used to obtain FASTQ files from the Illumina base call files, align the sequencing reads to the 10 mm mouse transcriptome reference using "intronic reads included" mode, and further quantify the expression level of transcripts in single-cells. Subsequent analyses were performed using R software v 4.3.2 and Seurat package v 5.0.1 [30]. Low-quality cells (cells expressing > 10% mitochondrial transcripts or number of transcripts < 200) and doublets (number of transcripts > 6000) were filtered out. Gene expression data was natural-log normalized. The top 2000 high-variability genes were selected using the 'FindVariableGenes' function. The gene expression data were then scaled and subjected to dimensionality reduction through Principal Component Analysis (PCA). To integrate cells from all samples, PCA embeddings were corrected using the Harmony package, version 1.2.0 [31]. For unsupervised clustering, the 30 nearest neighbors were identified by function 'FindNeighbors' based on Harmony adjusted PCA embedding. 'FindClusters' functions were further applied to identify cell clusters based on the Louvain algorithm. The identified clusters were visualized in Uniform Manifold Approximation and Projection (UMAP) embeddings which were calculated using the top 30 principal components. To accurately annotate cell types in the neonatal murine model, data from the more extensively studied young adult murine model was employed as a reference. This involved integrating neonatal sample data with young adult samples, which included samples from both healthy and septic animals. Cell types were manually annotated based on marker genes identified from the literature. Initially,

broad cell categories such as myeloid, lymphoid, DC and plasma cells were determined. Once these major groups were established, the myeloid cell compartment was further divided into subsets, following the unsupervised clustering process shown above within each cell cluster. For each cell type of interest, differential expression (DE) analysis across groups were performed using non-parametric Wilcoxon rank sum test with p-values adjusted by Bonferroni correction. Genes were identified as differentially expressed (DEGs) based on two criteria: an adjusted p-value of less than 0.001 and an absolute $\log_2$ fold change (FC) greater than 1. Marker genes were identified for each cell type by comparison to all others.

Methyltransferase Accessibility Protocol for Individual Templates combined with Flap-Enabled Next-Generation Capture (MAPit-FENGC) epigenetic analysis.

MAPit-FENGC is a validated method that allows for simultaneous single-molecular level analysis of methylation and accessibility at target promoter and enhancer regions[27]. 1 million cells from each mouse were washed with ice-cold PBS, pH 7.2. Cells were centrifuged at 1,000 *x g* for 5 min then washed in ice-cold cell resuspension buffer (20 mM HEPES pH 7.5, 70 mM NaCl, 0.25 mM EDTA pH 8.0, 0.5 mM EGTA pH 8.0, 0.5% glycerol, with freshly supplemented 10 mM DTT and 0.25 mM PMSF). Cells were centrifuged at 1,000 *x g* for 5 min before being resuspended with 92 µL of resuspension buffer with 0.5 % digitonin. Cells were then stained with trypan blue to ascertain 100 % permeabilization. The cells were then treated with 100 U M.CviPI GpC methyltransferase (100 U / million cells; New England Biolabs, M0227B-HI) with fresh 160 160 µM S-adenosyl-L-methionine for 15 min at 37°C. The reaction was terminated using an equal volume of 10 mM EDTA, 100 mM NaCl, and 1% (w/v) SDS followed by a quick vortex at medium speed. The nuclei were treated with 100 µg/ml RNase A for 30 min at 37°C followed with 100

μg/ml proteinase K treatment at 50°C overnight. Extraction of genomic DNA was conducted using phenol-chloroform-isoamyl alcohol (25:24:1, v/v) phase separation, which was followed by ethanol precipitation, then resuspension in molecular-grade H_2O. The full FENGC methodology can be found at Zhou et al. (2022)[27]. Target gene promoters and enhancers were located using the transcription start site (TSS) region and encode annotations from the mm10 genome assembly. Flap oligos 1 and 2 as well as the nested oligos 3 are catalogued in **Supplementary Material 1**. All three oligos (4 nmole each) were ordered as 0.3-mL each as salt-free oligos in 96 well format (Eurofins Genomics, KY, USA). Purified amplicons were submitted to the University of Florida Interdisciplinary Center for Biotechnology Research (UF-ICBR, RRID:SCR_019152) for SMRT bell library construction. Sequencing was run on PacBio SEQUEL IIe (City, State) instrument by UF-ICBR. The library pool was loaded at 120 pM, using diffusion loading and 20- to 30- h movies with HiFi generation and demultiplexing. Sequencing Kit 2.0 (PacBio, 101-389-001) and Instrument Chemistry Bundle Version 11.0 were used with all other steps being performed using recommended protocol by the PacBio sequencing calculator. For epigenetic analysis, high-fidelity circular consensus sequencing (CCS) was generated using default parameters except for a setting of ≥ 5 single polymerase read passes. CCS reads were aligned to the reference sequences using the python reAminator pipeline[32]. Cut-offs to 95% conversion rate and 95% length of reference sequences alignments were applied. To distinguish endogenous CG methylation and M.CviPI-probed GC methylation, the unambiguously GCG sites were removed from calculation of HCG and GCH methylation (where H is A, C, or T). Averaged heatmaps were constructed based on averaged percent HCG/GCH per nucleotide post-methylscaper analysis[33]. A total of 180 primers for selected promoter and enhancer regions of immune and trauma-related genes (**Supplemental Material 1**) were used to concurrently profile chromatin accessibility and methylation.

Principal Component Analysis (PCA) of Epigenetic Features

To assess global epigenetic differences in $CD11b^+$ $Gr1^+$ MDSCs isolated from murine spleens, we performed PCA on MAPit-FENGC-derived single-molecule data. Three types of data matrices were used: (1) endogenous CpG methylation (HCG sites), (2) GpC methylation representing chromatin accessibility (GCH sites), and (3) combined HCG + GCH profiles. For each sample, a matrix of percent methylation across covered sites was generated and filtered to retain loci with ≥25 informative reads. PCA was conducted using base R's prcomp() function without imputation. After quality filtering, each promoter target was filtered for fewer than 25 reads. Targets were not used in the PCAs if < 2 samples had data passing the filter. No female target promoters are missing in the PCAs, but these male promoters are missing: C3ar1, Car6, Ctsl, Igkv8-24, Il1r2, Irf8, and Tmem176a.

Results

Global Epigenetic Structure Separates MDSCs by Sepsis, Age, and Sex

Principal component analysis (PCA) of MAPit-FENGC data revealed clear global distinctions in the epigenetic landscape of $CD11b^+$ $Gr1^+$ splenic MDSCs based on sepsis exposure, age, and sex. In PCA of endogenous CpG methylation alone (**Figure 1**), septic mice formed distinct clusters compared to naïve controls. Notably, older adult females demonstrated the greatest divergence in methylation patterns after sepsis, suggesting age- and sex-dependent remodeling of the methylome. When PCA was restricted to GpC methylation (chromatin accessibility) data (**Figure 2**) and combined CpG and GpC clustering (**Figure 3**), sepsis again drove marked separation, particularly among female samples. Septic females (both young and older adult) clustered distinctly from their naïve counterparts, whereas MDSCs derived from all adult males displayed a

more intermediate shift. This suggests that chromatin accessibility is broadly altered by sepsis, with a stronger response in females.

Distinct Promoter Accessibility Classes exist in MDSCs Following Sepsis

Unsupervised analysis of the MAPit-FENGC data revealed nine promoter classes (Class 1–9) in splenic CD11b^{+} Gr1^{+} MDSCs, each with characteristic chromatin accessibility and DNA methylation patterns across conditions (**Table 1**). These classes capture the range of epigenetic responses to sepsis and underline strong age- and sex-specific differences in MDSC promoter regulation. Here, we describe qualitative trends for each class, highlighting how sepsis-induced chromatin accessibility (nucleosome-free regions, NFRs) and DNA methylation changes vary by promoter class, age, and sex.

1. Sepsis Induces Nucleosome-Free Regions at Many Promoters (Classes 1–4)

Several promoter classes exhibited marked chromatin opening in response to sepsis. A single Class 1 promoter, *S100a9* (encoding the alarmin calcium-binding protein A9), showed the most robust sepsis-driven increase in accessibility (at GCH sites; right; yellow color), forming large nucleosome-free regions (NFRs) in the majority of septic mice. The magnitude of NFR formation in Class 1 was modulated by sex and age. For example, the *S100a9* promoter (S100A9 is a key MDSC protein that regulates MDSC trafficking, expansion, and activation, as well as acting as an alarmin[34, 35] displayed a dramatic increase in accessibility after sepsis, with older females showing the largest NFRs and greatest fraction of molecules with NFRs (indicating a higher proportion of cells with an open promoter; **Figure 4**). In female MDSCs, old septic mice had significantly more extensive *S100a9* promoter opening than young septic females, whereas male MDSCs showed

robust *S100a9* NFR formation in sepsis regardless of age (though slightly less pronounced than in females). This Class 1 promoter had moderate DNA methylation at baseline that underwent partial demethylation upon sepsis, in line with an activated chromatin state. Together, the data indicate the Class 1 promoter is broadly inducible by sepsis, with female MDSCs (especially aged females) exhibiting the greatest increase in chromatin accessibility gains at these promoters.

Class 2 promoters also gained accessibility in septic conditions but in a more context-dependent manner. Specifically, Class 2 chromatin opened (NFRs appeared) in old female sepsis and in male sepsis (both young and old), but not in young female sepsis. This pattern indicates that young females failed to open these promoters unless aged, whereas males of either age mounted an increase in accessibility. When present, the degree of NFR formation for Class 2 genes was similar between sexes. A representative Class 2 gene is *Nos2* (encoding inducible nitric oxide synthase, iNOS, with nitric oxide (NO) subsequently inhibiting T cell function[36]: in septic MDSCs, the *Nos2* promoter remained nucleosome-occupied (by randomly positioned nucleosomes) in young females but showed clear NFR formation in old females and in males (both ages) (**Figure 5**). Concordantly, *Nos2* and other Class 2 promoters (e.g. *Cxcr2*, *Ptgs2*) exhibited low-to-moderate DNA methylation (at HCGs; left; red color) that either remained stable or slightly decreased with sepsis in the responsive groups. The requirement of advanced age for female MDSCs to demonstrate open Class 2 loci, *versus* no such requirement in males, highlights a female-specific age dependency in epigenetic activation of this promoter set. Importantly, the fact that young females showed robust Class 1 and Class 3 responses (see below) confirms that the lack of Class 2 accessibility in young female mice is not due to a weaker septic stimulus, but rather reflects a fundamental epigenetic sex difference. As shown in **Figure 5**, promoters like *Nos2* gained NFRs

only under the conditions noted above, underscoring a conditional sepsis response tied to both sex and age.

Class 3 promoters were broadly responsive to sepsis across all cohorts, with no significant sex or age differences in their accessibility changes. These loci (e.g. *S100a8* (S100A8 acts similarly to S100A9[34] and *Mmp8* (MMP8 facilitates MDSC mobilization and migration, as well as the immunosuppressive environment[37] formed NFRs in septic MDSCs in both males and females, and in both young and old mice, to a similar extent. As a result, Class 3 represents a core set of promoters that are consistently opened by sepsis irrespective of host age or sex. DNA methylation of Class 3 promoters was generally low to intermediate and showed modest changes (often slight demethylation) upon sepsis, if any. The uniform NFR formation at these sites suggests they may drive fundamental sepsis-responsive genes in MDSCs that are required in all populations. For instance, the *S100a8* (encoding encodes the S100 calcium-binding protein A8) promoter exhibited equivalent accessibility gains in septic males and females, young and old (**Figure 6**), mirroring the behavior of its Class 1 counterpart *S100a9*, but without the female-old bias. Similarly, *Mmp8* (encoding matrix metalloproteinase-8) opened consistently in all septic groups. Thus, Class 3 promoters highlight sepsis-induced epigenetic changes that are common to both sexes and ages, representing an invariant component of the MDSC response to sepsis.

In contrast, a single Class 4 promoter displayed a clear sex-specific accessibility pattern. This promoter, of *Fyb* (encoding adhesion and degranulation adaptor protein (ADAP), which is a signaling adaptive protein that is hypothesized to support MDSC migration, suppressive activity, and survival [38], demonstrated accessibility in old and young naïve mice; the promoter opened in

more MDSCs from septic female mice of both ages. In contrast, septic males (Old or Young) showed no detectable increase in chromatin opening beyond the initial accessibility of the *Fyb* TSS region in naïve male mice of both ages (**Figure 7**). Both young and old female MDSCs generated clear NFRs at Class 4 loci after CLP-induced sepsis, whereas male MDSCs retained nucleosome-occupied, inaccessible chromatin at these promoters. One example is the *Fyb* gene promoter which remained closed in septic males but underwent robust NFR formation in septic females. DNA methylation levels at the Class 4 *Fyb* promoter were rather low at baseline and showed further demethylation in female sepsis, especially in older mice, consistent with transcriptional activation in females. The absence of any chromatin change in males, despite an adequate sepsis insult (as verified by other classes), emphasizes a sex divergence in epigenetic regulation, with Class 4 loci preferentially activated in female MDSCs during sepsis.

2. Persistently Closed Promoters Remain Refractory to Sepsis (Class 5)

In contrast to the sepsis-inducible classes above, Class 5 promoters remained closed and nucleosome-bound under all conditions examined. Chromatin at these loci showed no formation of an NFR in any group (naïve or septic, male or female, young or old). Instead, the DNA was wrapped in randomly positioned nucleosomes, indicating a lack of organized accessibility. Class 5 promoters were generally characterized by high levels of DNA methylation (hypermethylation), which is consistent with a silenced state. Representative genes in Class 5 include *Lyz1* (lysozyme 1), *Retn* (resistin), and *F7* (coagulation factor VII), among others (**Figure 8**) These promoters showed minimal change in methylation or accessibility after sepsis. For example, the *Lyz1* promoter remained densely methylated and completely inaccessible in both control and septic

MDSCs. Similarly, *Retn* showed no NFR formation in any condition, and although its methylation level dropped slightly in old sepsis compared to old naïve.

3. Age-dependent loss of accessibility in Old Septic Mice (Classes 6–8)

We identified several promoter classes where chromatin accessibility was present in certain baseline or younger conditions but was lost specifically in MDSCs from older septic mice. Classes 6, 7, and 8 represent promoters that underwent a sepsis-specific closure exclusively in older mice, highlighting an age-driven epigenetic effect opposite to the opening seen in other classes. In these cases, older mice subjected to sepsis failed to maintain promoter accessibility that was observed in young mice or in non-septic controls.

Class 6 and Class 7 promoters were initially in a relatively accessible or poised state (some exhibiting NFRs or organized chromatin) in young and/or naïve mice, but in old septic mice these loci became fully closed (no detectable NFRs, only randomly positioned nucleosomes). The distinction between Class 6 and 7 lies in their DNA methylation status: Class 6 promoters had moderate-to-high CpG methylation (often showing little to no demethylation), whereas Class 7 promoters had low baseline methylation. Despite these differences, both classes demonstrated an older sepsis-specific loss of accessibility. For example, the *Serpine1* promoter (**Figure 9**; encoding the fibrinolytic serine protease inhibitor Pai-1 protein, which influences the presence and activity of MDSCs often promoting immunosuppression and tumor growth [39] possessed an open chromatin configuration in younger mice, but in MDSCs from older septic mice it lost NRFs. This was accompanied by some changes in DNA methylation; notably, MDSCs from older septic mice

showed demethylation at *Serpine1* CpGs compared to young sepsis or old naïve mice yet the chromatin remained closed. Another example is the *Vcan* gene (**Figure 10**; Class 7) that encodes Versican, an extracellular matrix component that is upregulated during sepsis and thought so have some immune regulatory properties[40, 41]. Another Class 7 promoter is Il10 (that encodes the anti-inflammatory cytokine interleukin 10; data not shown) promoter. MDSCs are producers of and responders to IL10, which enhances their ability to immunosuppress [42]. *Vcan* and *Il10* in younger or naïve mice displayed partial accessibility (consistent with low DNA methylation at its promoter), but in MDSC from older septic mice these promoters were completely inaccessible, lacking any NFRs. The loss of even a partially open state of Class 7 promoters in MDSC from older septic mice implies a failure to induce these immunoregulatory genes.

Class 8 gene promoters illustrated this age-dependent trend in a particularly clear way, with significant accessibility in three out of four conditions (MDSC from young naïve, young sepsis, and old naïve mice), but underwent a complete loss of accessibility in MDSC from older septic mice. In other words, these promoters were open and presumably active except when an older mouse underwent sepsis. Class 8 promoters generally started with low DNA methylation levels, reflecting their active status, and underwent further DNA demethylation in old septic mice despite losing chromatin accessibility. An example of Class 8 is the *Cd274* gene (**Figure 11A-B**), which encodes the immune-checkpoint inhibitor immune checkpoint PD-L1, which in MDSCs plays a direct role in suppressing T cell responses[43]. The *Cd274* promoter was accessible (contained NFRs) in MDSCs from young septic mice as well as in old naïve controls, but in old septic MDSCs the promoter NFRs disappeared, indicating nucleosome occupancy and transcriptional silencing. Correspondingly, CpG methylation at the *Cd274* promoter was significantly reduced in MDSCs

from old septic mice compared to old naïve (and young septic) mice, suggesting active DNA demethylation occurred even as the chromatin condensed (a discordant epigenetic change). Other Class 8 genes, such as *Nfkbiz* (encoding the NF-κB inhibitor IκBζ; **Figure 11C-D**), *Vdr* (vitamin D receptor), *Il4ra* (IL-4 receptor α chain, which has been shown to be important to MDSC suppressive activity[44]), and *Atf6* (AFT6, a transcription factor that activates target genes for the unfolded protein response) all followed a similar pattern with NFRs present in all conditions except old septic mice. In each case, MDSCs from the old septic group showed a unique loss of promoter accessibility, often coupled with demethylation. These data indicate that MDSCs from aged mice experience a unique epigenetic shutdown of certain promoters during sepsis, which is not seen in younger adults.

4. Constitutively accessible promoters that maintain open chromatin in all conditions (Class 9)

Finally, a small subset of promoters (Class 9) remained highly accessible across all conditions, largely unaffected by sepsis, age, or sex. Class 9 promoters had pre-existing nucleosome-free regions in naïve MDSCs and retained these open states after the stress of sepsis. They also displayed low basal DNA methylation, consistent with active promoters, and in some cases showed further demethylation in old sepsis despite already being open. A clear example is the *Tet2* promoter, which encodes the DNA demethylation enzyme TET2 (**Figure 12**). The *Tet2* promoter showed prominent NFRs in all samples across all conditions indicating constitutive chromatin accessibility (likely reflecting ongoing expression of *Tet2* in MDSCs). Notably, analyzed promoters from MDSC from older septic mice were even more demethylated at CpG sites relative to MDSCs from young sepsis or old naïve, though its accessibility was already maximal. This

suggests that sepsis in aged mice can reinforce the active epigenetic state of certain always-on genes in MDSCs.

Single-cell transcriptomics support epigenetic promoter class distinctions in MDSC subsets

To determine whether promoter accessibility classes defined by MAPit-FENGC corresponded to functional gene expression patterns, we analyzed single-cell RNA-seq data from $CD11b^{+}Gr1^{+}$ splenic leukocytes isolated from young and old, male and female mice under naïve or septic conditions. Data were stratified into three myeloid-derived suppressor cell (MDSC) subtypes: early MDSCs (E-MDSC), monocytic MDSCs (M-MDSC), and polymorphonuclear MDSCs (PMN-MDSC). The gene *S100a9* was assigned as a Class 1 promoter, characterized by widespread NFR formation in all septic groups, exhibited induction across all three MDSC subsets in response to sepsis, regardless of age or sex (**Figure 13**). This transcriptional profile matches the broadly accessible chromatin configuration observed epigenetically. Similarly, the Class 3 promoter *S100a8*, which are accessible across all conditions, displayed upregulation in E-MDSCs and PMN-MDSCs during sepsis. In contrast, a Class 7 promoter *Ccl5*, which remained epigenetically inaccessible in all conditions, showed only modest and selective transcriptional induction in a subset of MDSCs, primarily E- and M-MDSCs, in young male septic mice (**Figure 14)**. These observations are consistent with a transcriptionally repressed or enhancer-driven regulatory program. In contrast, *Nfkbiz*, assigned to Class 8 based on selective promoter closure in "Aged Sepsis" despite DNA demethylation, showed relatively low but detectable expression across MDSC subsets. While MAPit-FENGC revealed loss of promoter accessibility specifically in aged

sepsis mice, scRNA-seq analysis did not show consistent transcriptional silencing in this group. Instead, modest expression changes were observed in PMN-MDSCs and E-MDSCs, particularly in young female septic mice. *Tet2*, a representative Class 9 gene whose promoter remained consistently accessible across all MAPit-FENGC conditions, exhibited modest transcriptional activation in scRNA-seq, limited primarily to sepsis conditions in M-MDSCs (**Figure 15)**. Despite the stable chromatin accessibility across all groups, expression was low or unchanged in E-MDSCs and PMN-MDSCs.

Discussion

Our study provides the first high-resolution, single-molecule epigenetic map of MDSC in a murine model of surgical sepsis, revealing how host age and sex shape chromatin accessibility and DNA methylation in this immunoregulatory cell type. Using MAPit-FENGC, we identified nine distinct promoter classes across multiple immune-relevant loci, encompassing a spectrum of response classes ranging from sepsis-induced chromatin opening to age-specific silencing. These epigenetic

patterns were tightly linked to host sex, age, and sepsis exposure and corresponded to transcription as assessed by scRNA-seq.

We discovered an age-dependent epigenetic repression of key immunoregulatory genes (e.g., *Cd274*, *Nfkbiz*, *Il4ra*) in older septic mice (Classes 6-8). These genes exhibited robust promoter accessibility in young or naïve mice but became transcriptionally inaccessible in MDSCs from older septic animals despite persistent or even reduced CpG methylation. This discordance highlights a decoupling between DNA methylation and chromatin accessibility, with nucleosome repositioning emerging as the dominant mechanism of transcriptional repression in aged MDSCs. The selective closure of immune checkpoint and anti-inflammatory loci (e.g., *Cd274*, *Il10*) may impair key MDSC functions (T cell suppression and inflammation resolution) which rely on PD-L1 and IL-10 expression. In aged septic hosts, epigenetic repression of these genes may render MDSCs less effective or dysregulated, contributing to the persistent immune dysfunction and chronic critical illness seen in this population [16, 21].

In contrast, sepsis-induced chromatin opening was observed in promoter classes associated with canonical MDSC effector genes (Classes 1-4). Promoters such as *S100a9*, *S100a8*, *Nos2*, and *Ptgs2* gained accessibility in septic MDSCs, often with concurrent demethylation, consistent with transcriptional activation[34, 36]. The magnitude of these chromatin changes varied by sex and age. For example, Class 1 (*S100a9*) was accessible across all septic groups but showed particularly robust NFR formation in older females. These findings suggest that both age and sex can influence S100a9 expression and chromatin accessibility, potentially contributing to the observed robust NFR formation at the S100a9 promoter in older females during sepsis. Research has demonstrated

that chromatin accessibility at the S100a9 promoter is regulated during monocyte differentiation, and is influenced by transcription factors such as C/EBPδ. In particular, C/EBPδ has been shown to bind within the S100a9 promoter region, affecting its accessibility and expression levels[45]. Age-related changes in immune function ("inflammaging") have been associated with alterations in inflammatory markers, including S100a9. For example, a study investigating the impact of age and sex on inflammatory markers found that aging is associated with higher expression of *S100a9* and components of the NLRP3 inflammasome independent of sex[46]. In the context of systemic lupus erythematosus (SLE), S100a9 has been identified as a molecule integral in determining sex-specific immune responses[35], which may be relevant to understanding its regulation in other inflammatory conditions like sepsis.

Class 2 promoters opened only in older females and males, but not young females highlighting a female-specific age threshold for epigenetic activation at specific loci. For example, CXCR2 is a chemokine receptor primarily expressed on neutrophils and plays a crucial role in mediating their recruitment to sites of infection, essential for survival in sepsis. Excessive or dysregulated CXCR2 signaling can contribute to tissue damage and organ failure[47], and the observed increased accessibility of the CXCR2 gene in older females and males may suggest an age-related epigenetic regulation leading to enhanced expression.

The identification of stably closed promoters (Class 5) and constitutively open loci (Class 9) may further describe the epigenetic plasticity in MDSCs. Class 5 genes (e.g., *Lyz1*, *F7*) remained silenced regardless of condition. The refractoriness of Class 5 promoters to opening indicates they are epigenetically "locked down" in splenic MDSCs. These genes remain transcriptionally inactive

even in sepsis, suggesting they are either irrelevant to the MDSC sepsis response or otherwise tightly repressed in this cell type.

Classes 6-8 highlight an age-specific epigenetic repression: promoters that younger MDSCs can keep open are instead shut down in older MDSCs following sepsis. This finding points to an epigenetic basis for some of the differential gene expression profiles observed in old vs. young sepsis survivors. Across Class 6/7 promoters, we frequently observed that all MDSC samples from older septic mice lacked NFRs, whereas one or more of the other conditions retained an accessible configuration, suggesting age-specific chromatin condensation at these promoters. Class 8 includes several immune-related genes (e.g., *Cd274*, *Il4ra*, *Nfkbiz*) whose suppressed accessibility in older survivors of sepsis might contribute to impaired or altered immune regulation in this cohort.

Class 9 promoters (e.g., *Tet2*) were persistently accessible and low in methylation across all groups, suggesting these are "core" MDSC genes that remain transcriptionally poised or active even in the face of sepsis-induced stress, are simply important for the development of this cell type (the demethylation enzyme TET2 is highly expressed in hematopoietic stem and progenitor cells and has been shown to be essential in regulating MDSC numbers in tumor models[48] and models of emergency myelopoiesis post-LPS-challenge[49]). Generally, Class 9 genes appear to be core functional genes whose promoter chromatin is stably open as part of the identity or necessary function of MDSCs. Their invariant accessibility is in contrast to the dynamic changes seen in Classes 1-8. The presence of Class 9 promoters underscores that some key promoters remain epigenetically unaltered and continuously active throughout sepsis. Maintenance of an NFR at the

Tet2 promoter in all conditions exemplifies this stability. We did not observe any loss of accessibility at Class 9 loci, reinforcing that these promoters are resilient to both inflammatory stress and host factors.

These context-specific activation patterns suggest that MDSC-mediated immunosuppression may arise *via* different regulatory programs in males versus females, and in young versus old hosts. This observation aligns with our prior data on age- and sex-specific differences in MDSC transcriptomes and function[17, 19], and may provide mechanistic insight into how such differences are epigenetically encoded.

Importantly, single-cell transcriptomics supported many of the epigenetic patterns described. Genes in Classes 1 and 3 showed increased expression in MDSC subsets concordant with sepsis-induced chromatin opening. In contrast, Class 8 genes (e.g., *Nfkbiz*, *Il4ra*) showed partial decoupling between accessibility and expression in old septic MDSC raising the possibility of additional regulatory checkpoints, such as enhancer silencing or post-transcriptional control, particularly in aged immune cells[13, 26]. These findings underscore the importance of integrating multiple levels of gene regulation (chromatin state, methylation, and transcription) when evaluating MDSC behavior in critical illness. Collectively, these scRNA-seq results support the biological relevance of the MAPit-defined promoter classes, and illustrate how chromatin accessibility states correspond to transcriptional outcomes across sepsis, sex, and age in MDSC subsets.

The epigenetic heterogeneity observed here helps explain the divergent immune phenotypes / endotypes that we[50, 51] have defined in sepsis survivors, and provides a foundation for understanding MDSC dysfunction in aging. In particular, the age-specific silencing of checkpoint and anti-inflammatory loci may promote persistent immune suppression, a hallmark of chronic critical illness and poor sepsis recovery[4, 16]. Conversely, sex-biased promoter accessibility could underlie known disparities in sepsis outcomes between males and females[18]. These mechanistic insights may guide future strategies to therapeutically reprogram MDSCs using epigenetic modulators such as histone deacetylase (HDAC) inhibitors, bromodomain inhibitors, or DNA methyltransferase inhibitors, many of which are already being explored in oncologic and inflammatory contexts[7, 26].

Moreover, promoter classes defined here could serve as biomarkers of MDSC-state or targets for selective modulation. For instance, genes in Classes 1-3 may be used to identify actively suppressive MDSCs post-sepsis, while Class 8 promoters might be harnessed to identify aged immune populations with impaired regulatory function. The stability of Class 9 loci suggests they may serve as internal controls or indicators of MDSC identity in future epigenetic studies.

Our findings provide mechanistic insight into how sepsis may drive divergent epigenetic fates in MDSCs that reflect hallmarks of both trained immunity and tolerance. The persistent chromatin accessibility observed at Class 1-3 promoters (e.g., *S100a9*, *Nos2*, *S100a8*), particularly in older or female hosts, suggests a form of innate immune training, where prior inflammatory exposure leaves a molecular imprint that primes these loci for rapid reactivation. This is consistent with studies showing that chromatin remodeling at promoters of inflammatory genes underlies the

trained phenotype in monocytes and macrophages (reviewed in[52]). Conversely, the selective silencing of promoters in Classes 6-8, including key regulatory genes such as *Cd274* and *Il10*, supports the emergence of an epigenetic tolerance program, particularly in aged MDSCs. These loci become refractory to activation despite hypomethylation, implicating nucleosome repositioning and chromatin compaction as dominant suppressive mechanisms. The coexistence of both accessibility gains and repressive remodeling across promoter classes indicates that sepsis induces a divergent epigenetic landscape in MDSCs, poising some genes for increased responsiveness while silencing others. These dual trajectories may underlie the paradoxical state of immune hyperinflammation coupled with functional suppression seen in sepsis survivors, and reflect an imprint of the inflammatory milieu on the myeloid epigenome that varies by age and sex.

Limitations of this study are numerous. This study focused on a pre-selected set of immune and MDSC-relevant promoters, limiting discovery of unanticipated regulatory regions or enhancer-driven transcription. Additionally, while we profiled $Gr1^{+}CD11b^{+}$ cells, these include multiple MDSC subtypes and potentially other myeloid cells. Although single-cell RNA-seq helped disaggregate subtype-specific effects, future studies using single-cell epigenomics (e.g., scATAC-seq or scCUT&Tag) could more finely resolve MDSC heterogeneity[53]. Finally, the MAPit-FENGC approach provides high-resolution data at selected promoters but does not capture distal regulatory elements, which may play significant roles in aging-related immune dysfunction.

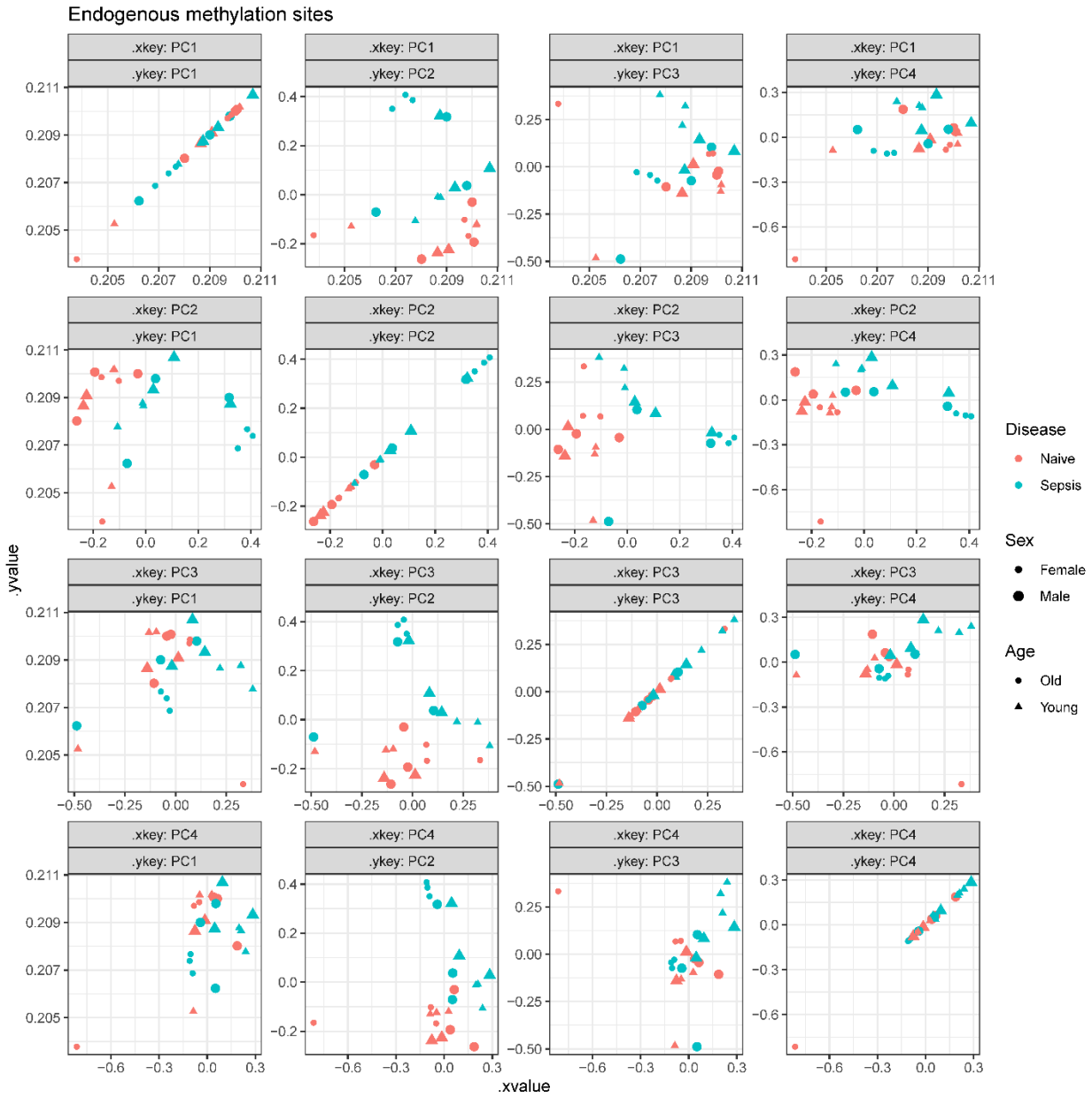

Figure 1. Principal component analysis (PCA) of endogenous CpG methylation (HCG) in splenic MDSCs. PCA was performed on the percent methylation of CpG (HCG) sites across all covered promoters in CD11b^{+} Gr1^{+} MDSCs from male and female mice, young and old, with or without sepsis. Each point represents a single mouse. Color indicates disease condition (blue = naïve, red = sepsis), shape denotes sex (circle = female, triangle = male), and shading differentiates age (light = young, dark = old). Principal components 1–4 are plotted in pairwise combinations to

visualize clustering. Old septic females exhibit distinct separation, indicating strong methylome remodeling in response to sepsis.

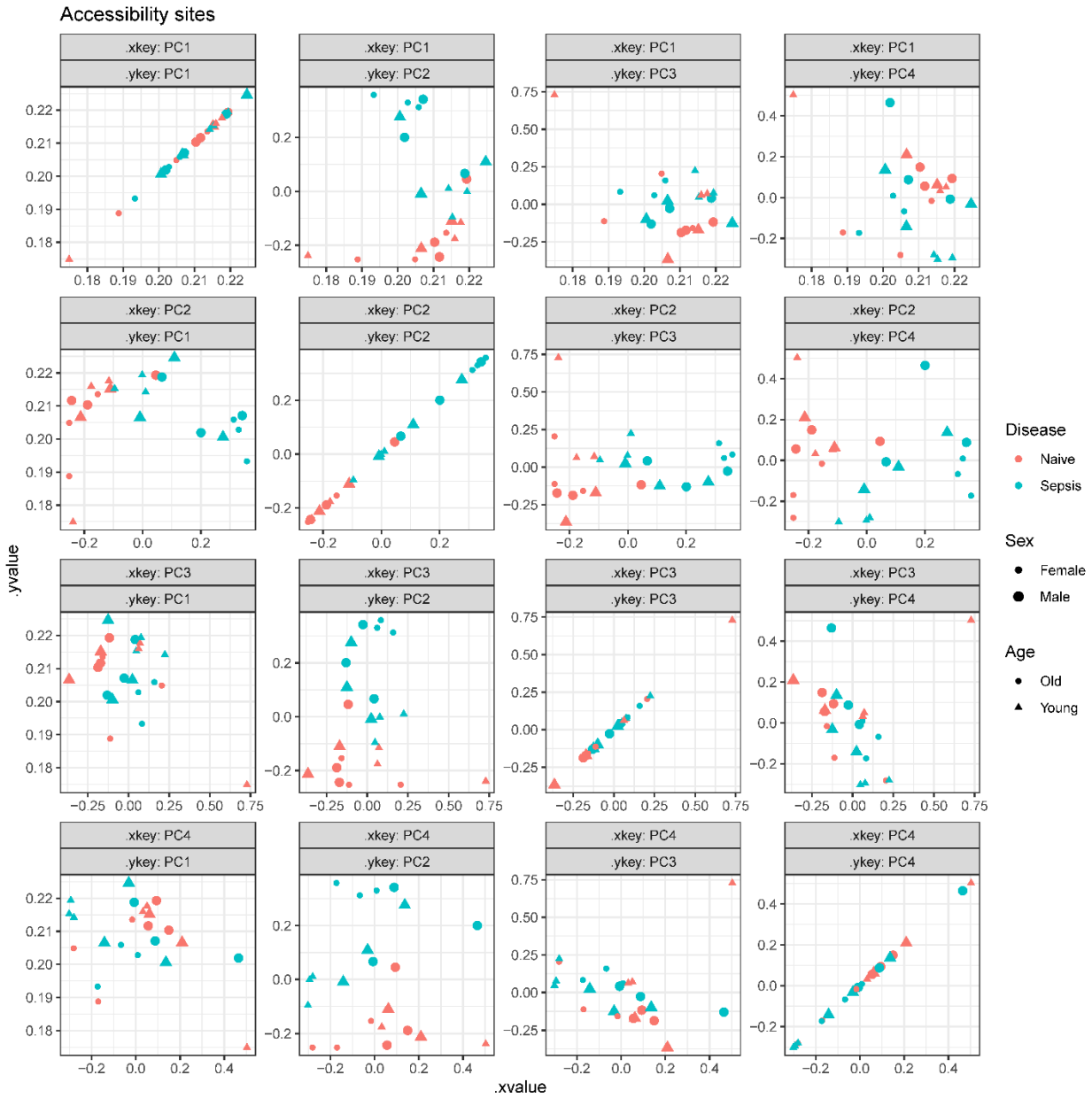

Figure 2. Principal component analysis (PCA) of GpC methylation (chromatin accessibility) in splenic MDSCs. PCA was performed using GCH methylation values from MAPit-FENGC to reflect promoter accessibility across MDSC samples. Each point represents a single mouse. Color indicates disease condition (blue = naïve, red = sepsis), shape denotes sex (circle = female, triangle

= male), and shading differentiates age (light = young, dark = old). Separation by sepsis status is evident across multiple PCs, with the strongest divergence observed in female mice. These results suggest widespread chromatin remodeling following sepsis, particularly in females.

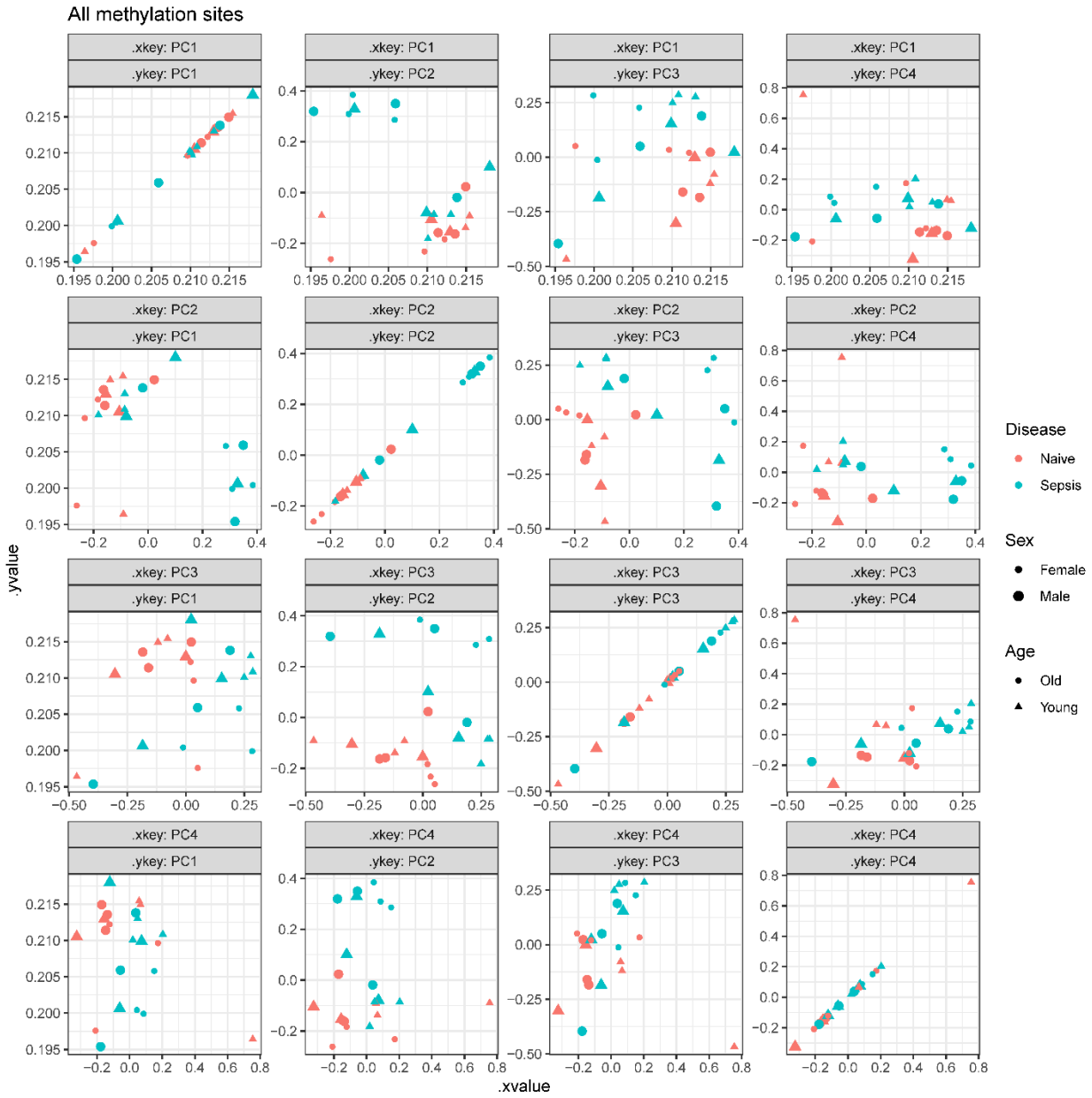

Figure 3. Principal component analysis of combined CpG and GpC methylation in splenic MDSCs. A joint PCA integrating both endogenous CpG methylation and in vitro GpC accessibility was performed to assess overall epigenetic structure in MDSCs. Each point represents a single mouse. Color indicates disease condition (blue = naïve, red = sepsis), shape denotes sex (circle = female, triangle = male), and shading differentiates age (light = young, dark = old). This

combined analysis yielded clearer separation across groups, especially for old female septic mice, suggesting coordinated reprogramming of both methylation and chromatin accessibility after sepsis. This integrated signature highlights how age and sex shape epigenetic responses to critical illness.

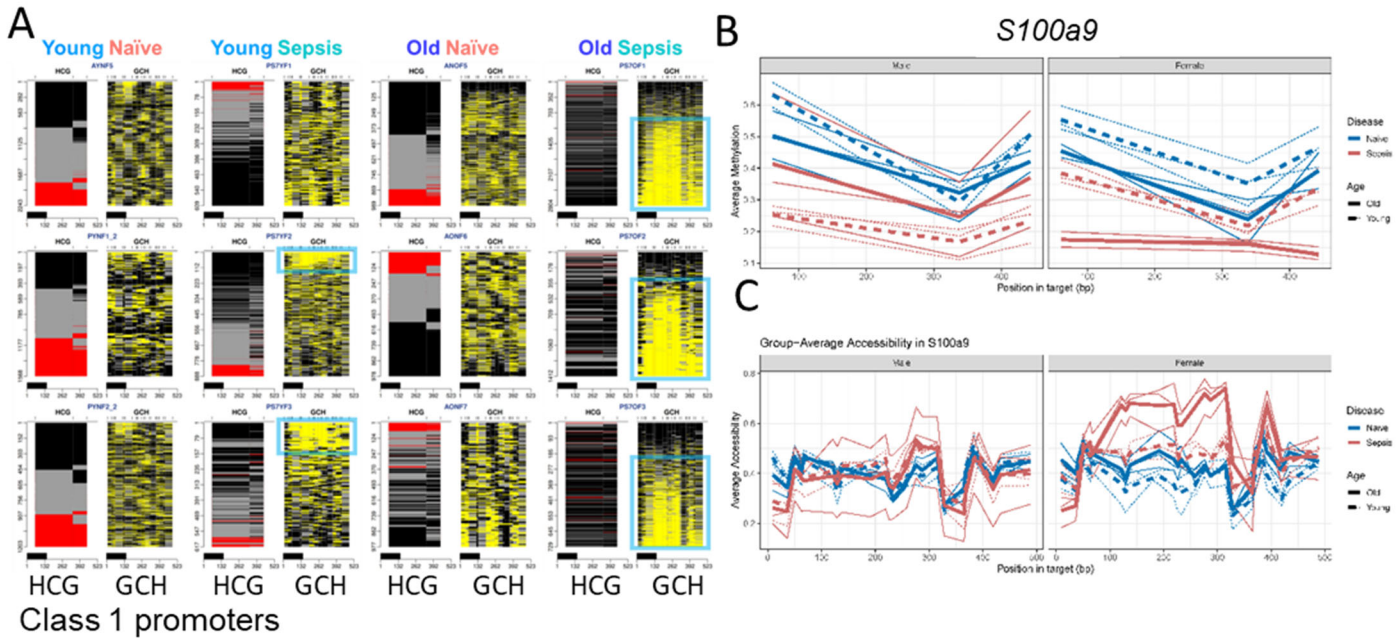

Figure 4. Class 1 promoters exhibit robust sepsis-induced chromatin accessibility and partial demethylation across MDSC subsets, with age- and sex-specific differences most evident at the S100a9 promoter. A) Representative single-molecule MAPit-FENGC plots for selected Class I promoters, showing simultaneous profiling of endogenous CpG methylation (HCG, left of each pair) and in vitro GpC methylation (GCH, right of each pair) in Gr1^{+} MDSCs from four experimental groups: Young Naïve, Young Sepsis, Old Naïve, and Old Sepsis all from female mice. Each horizontal line represents a unique DNA molecule. Black and gray marks denote methylated cytosines, while yellow marks indicate unmethylated (open or accessible) cytosines. Promoters are organized by gene and condition; Class 1 promoters were defined by consistent nucleosome-free region (NFR) formation in all septic groups. Blue boxes highlight particularly robust NFRs observed in *Old Sepsis* conditions, especially in females. **B)** Group-averaged endogenous CpG methylation levels across the *S100a9* promoter, plotted separately for males (left) and females (right). Sepsis (blue lines) induces partial demethylation relative to

naïve controls (red lines), with the most pronounced effects seen in *Old Female Sepsis* samples (solid blue line, right panel). **C)** Group-averaged chromatin accessibility (GpC methylation) across the same *S100a9* region, separated by sex.

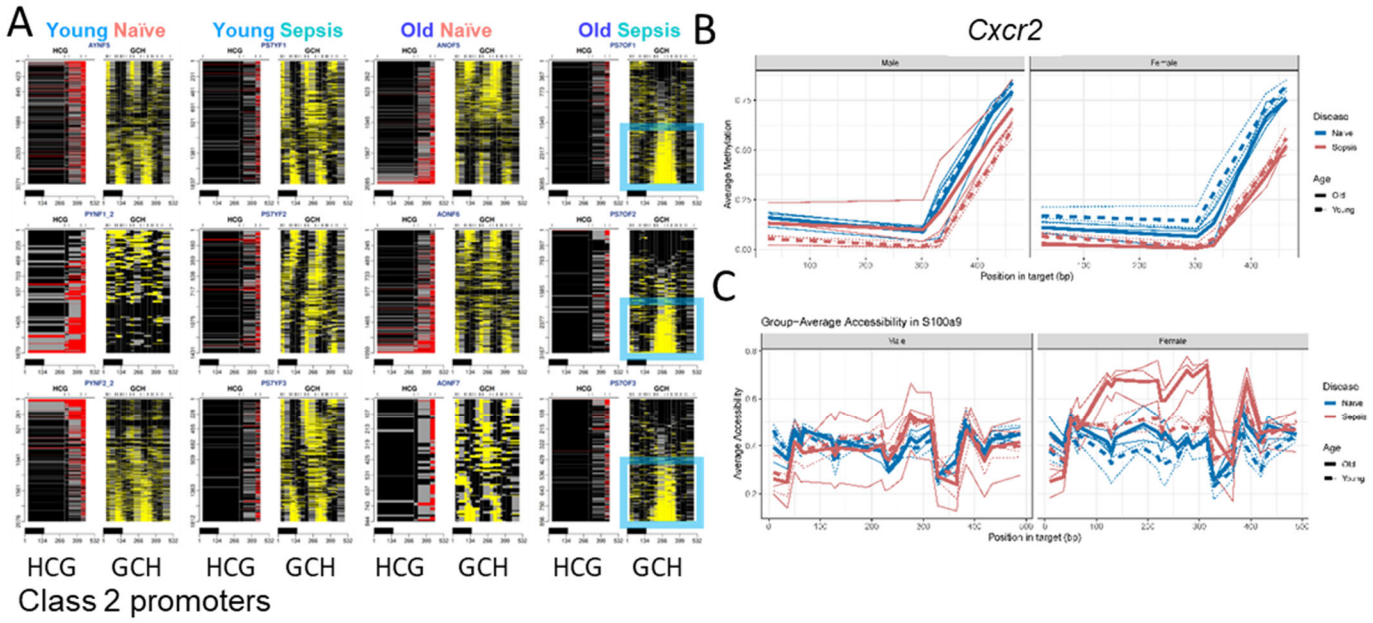

Figure 5. Class 2 promoters exhibit sex- and age-specific activation patterns, with sepsis-induced accessibility confined to Old Female and Male MDSCs. A) Representative single-molecule MAPit-FENGC plots of HCG (left) and GCH (right) profiles for Class 2 promoter genes (e.g., *Cxcr2*, *Nos2*) in Gr1^{+} MDSCs from Young and Old, Naïve and Sepsis Female mice. The Figure is annotated as in Figure 3. **B)** Group-averaged endogenous CpG methylation (HCG) across the *Cxcr2* promoter. Partial demethylation is observed in Old Female Sepsis compared to Naïve. **C)** Group-averaged chromatin accessibility (GpC methylation, GCH) at the same promoter. Old Female Sepsis shows increased accessibility, consistent with NFR formation and gene activation.

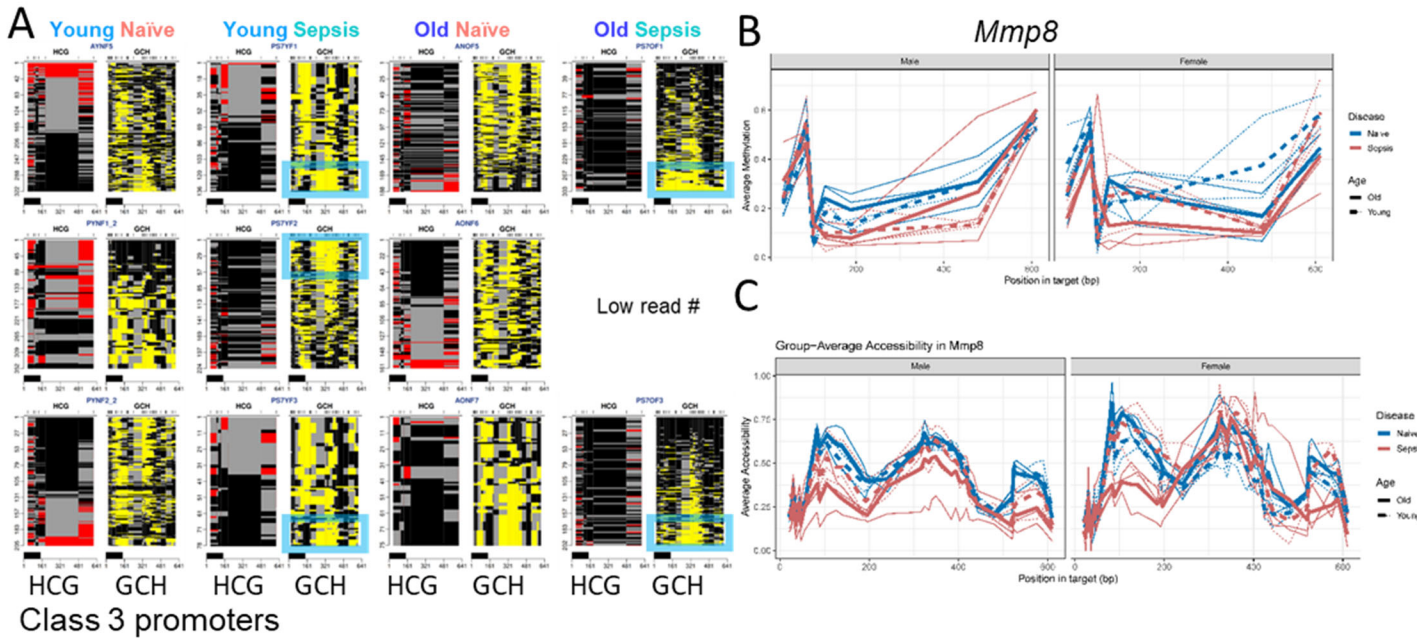

Figure 6. Class 3 promoters are consistently accessible in sepsis across all age and sex groups. A) Single-molecule MAPit-FENGC plots for Class 3 genes (e.g., *Mmp8*), showing HCG (left) and GCH (right) signals across Young/Old Female MDSCs. Sepsis induces NFRs in all septic conditions, regardless of age. The Figure is annotated as in Figure 3. **B)** Group-averaged CpG methylation (HCG) at the *Mmp8* promoter indicates minimal change with sepsis. **C)** Average GCH profiles show strong accessibility induction with sepsis across all age groups, supporting a core sepsis response program.

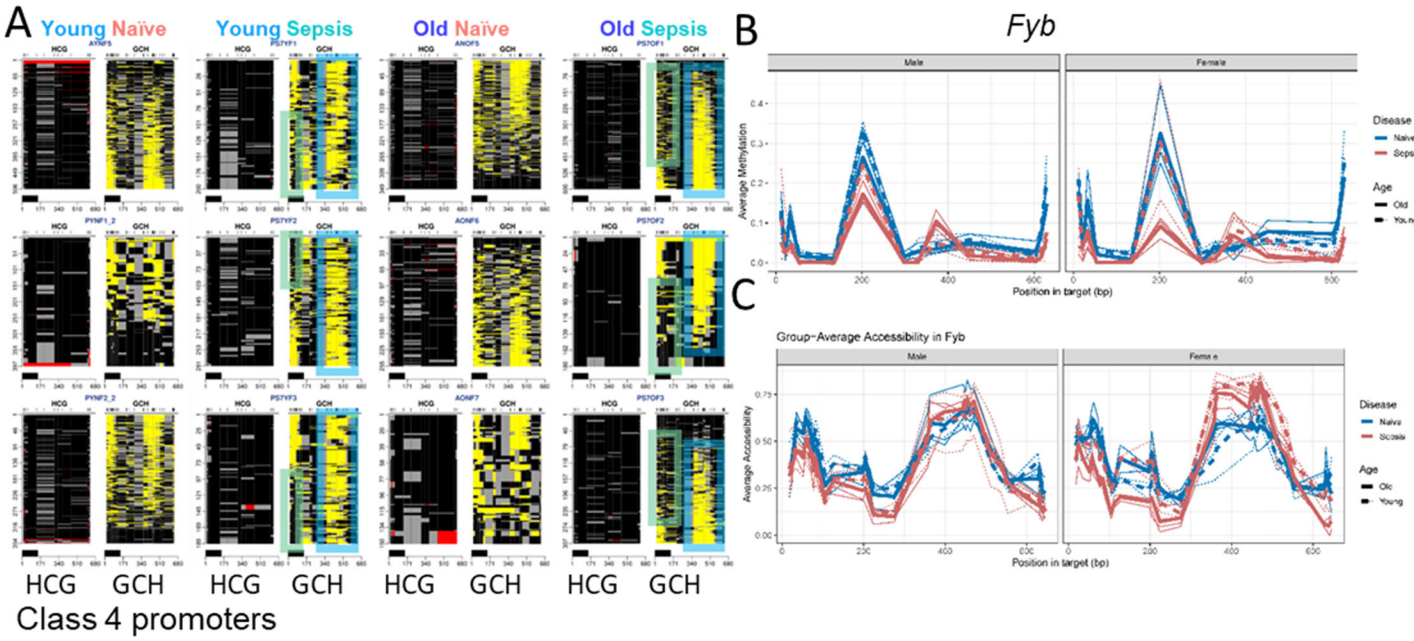

Figure 7. Class 4 promoters are activated by sepsis in females only. A) Single-molecule HCG and GCH plots for the *Fyb* promoter in Female MDSCs. NFRs appear in Young and Old Sepsis but are absent in Naïve conditions. The Figure is annotated as in Figure 3. **B)** Group-level HCG methylation at *Fyb* is moderately reduced in sepsis. **C)** GCH profiles show increased accessibility in both Female Sepsis groups.

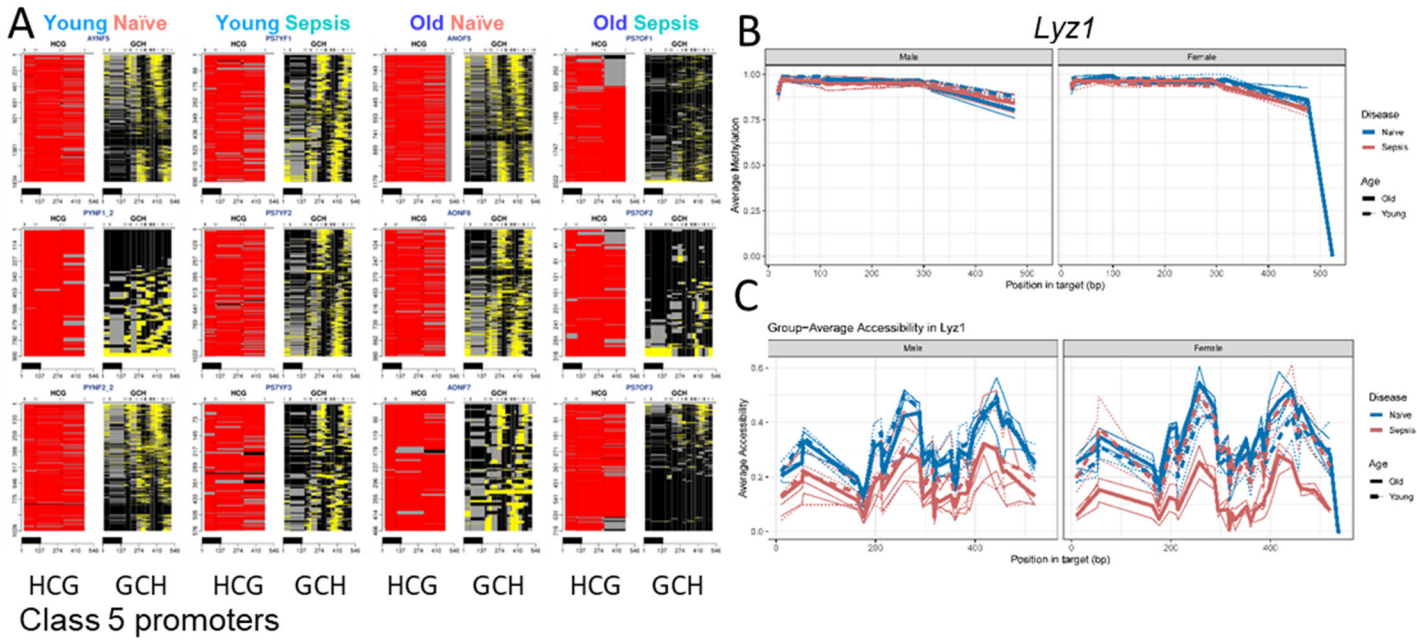

Figure 8. Class 5 promoters remain epigenetically silenced across all conditions. A) MAPit-FENGC plots of *Lyz1* showing no detectable NFRs in any condition. HCG and GCH signals indicate high methylation and random nucleosome positioning. The Figure is annotated as in Figure 3. **B)** CpG methylation at *Lyz1* is modestly reduced in Old Sepsis but remains high. **C)** GCH data show no chromatin opening, indicating persistent promoter repression despite inflammatory stimuli.

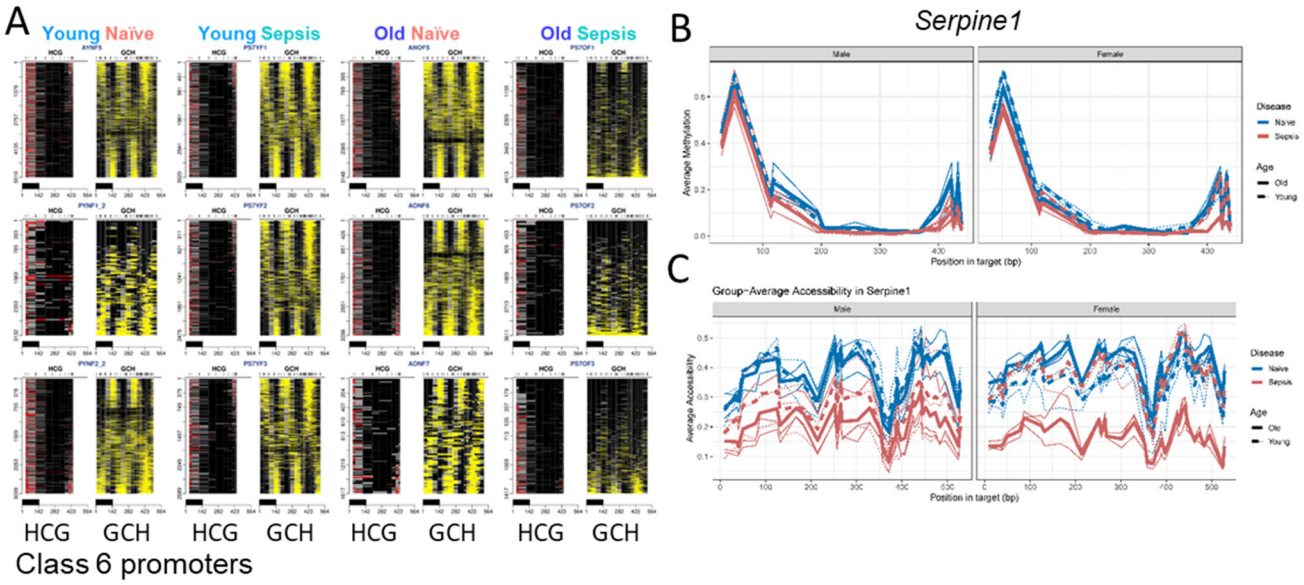

Figure 9. Class 6 promoters lose accessibility in Old Sepsis only. A) Single-molecule HCG and GCH plots for the *Serpine1* promoter show chromatin accessibility in all conditions except Old Sepsis, where NFRs are lost. The Figure is annotated as in Figure 3. **B)** CpG methylation decreases in Old Sepsis, paradoxically accompanying reduced accessibility. **C)** GCH accessibility is diminished in Old Sepsis, indicating sepsis-specific chromatin closure in aged mice.

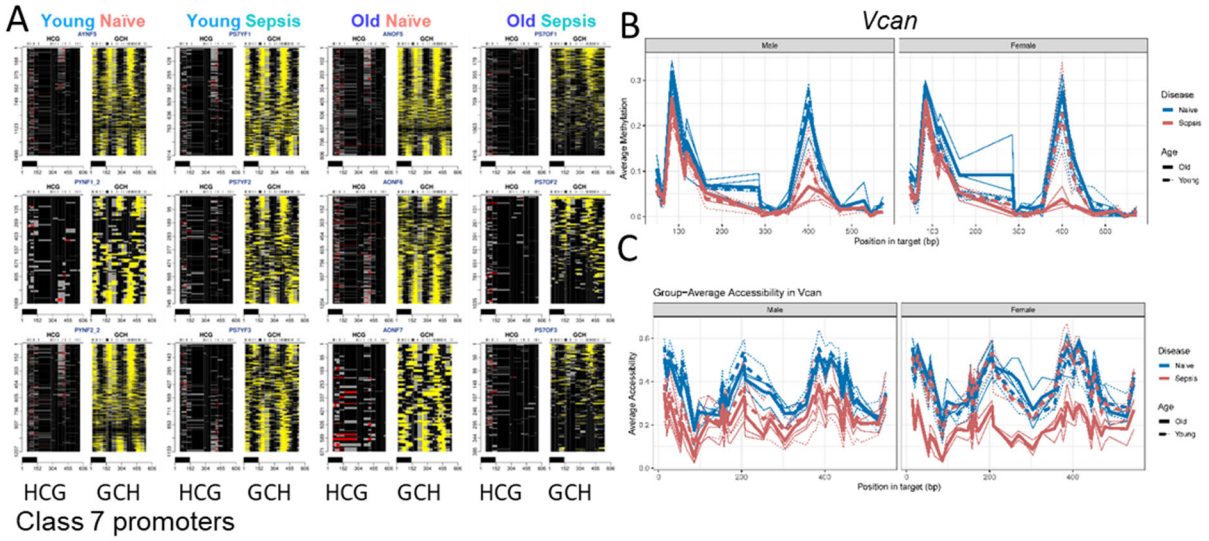

Figure 10. Class 7 promoters are consistently inaccessible but vary in DNA methylation. **A)** HCG and GCH plots for *Vcan* promoter show a complete lack of NFRs across all female conditions. The Figure is annotated as in Figure 3. **B)** CpG methylation is low to moderate, with minor demethylation in some septic conditions. **C)** GCH profiles confirm uniformly closed chromatin, indicating transcriptional silence across all age and sepsis states.

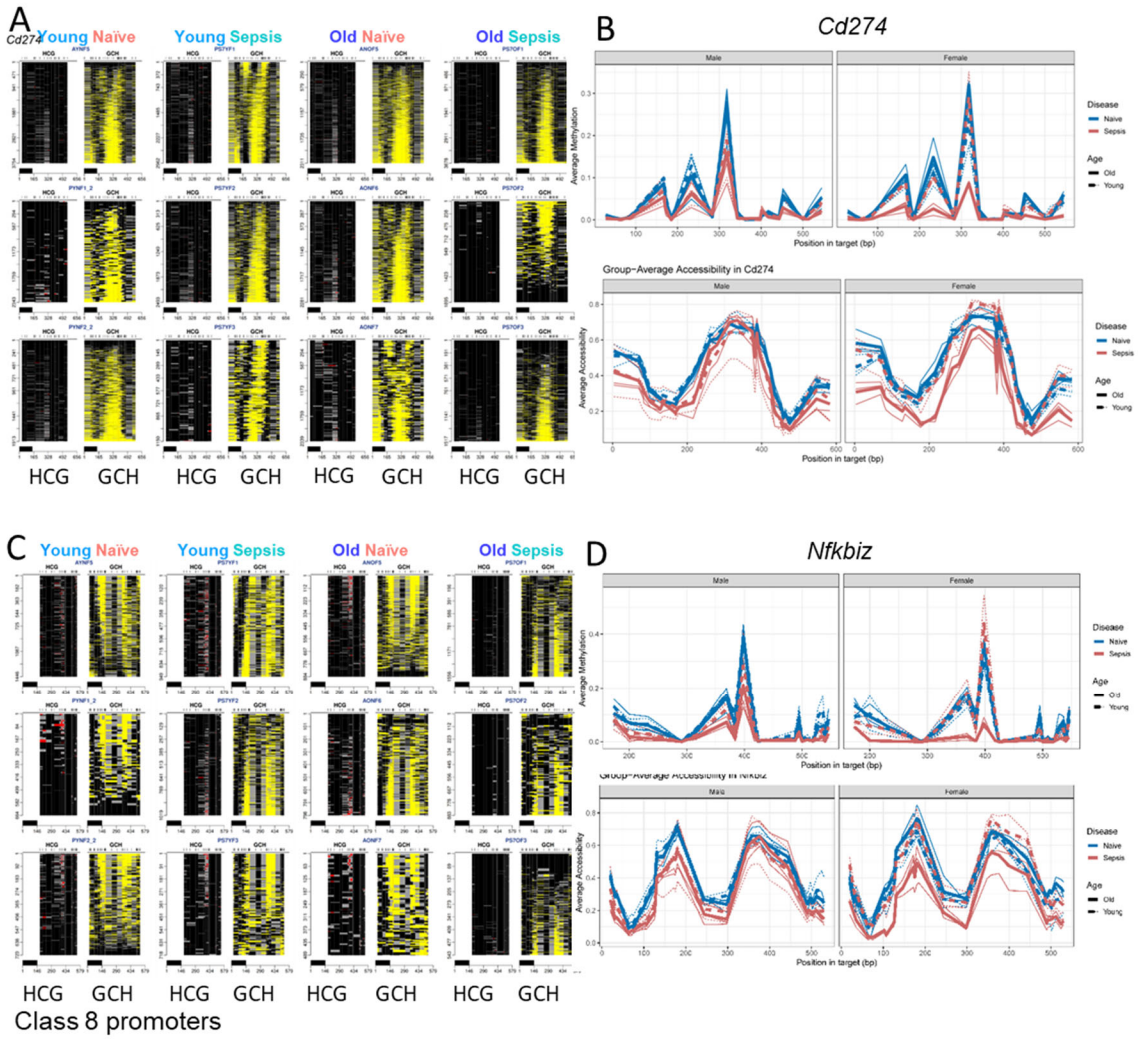

Figure 11. Class 8 promoters lose accessibility specifically in Old Sepsis. A) MAPit-FENGC plots for *Cd274 (***A-B**) and *Nfkbiz* (**C-D**) and show NFRs in all groups except Old Sepsis. The Figure is annotated as in Figure 3. **B,D)** CpG methylation is reduced in Old Sepsis mice, even as accessibility declines, GCH plots reveal a complete loss of NFRs in Old Sepsis, despite prior openness, pointing to age-dependent epigenetic silencing.

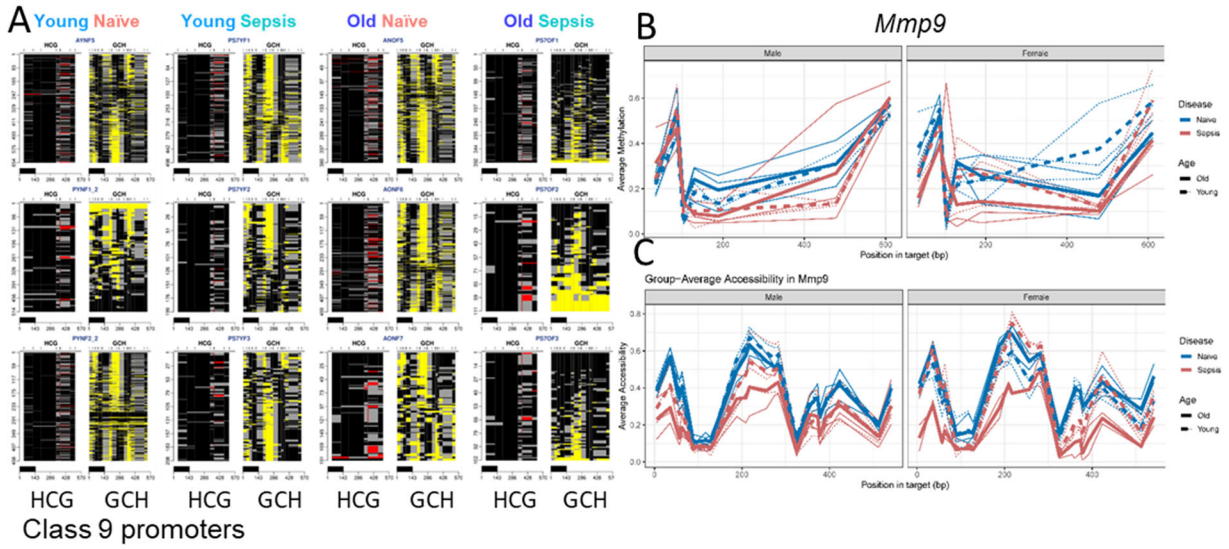

Figure 12. Class 9 promoters are constitutively open with increased demethylation in sepsis. A) HCG and GCH plots for the *Tet2* promoter show strong, stable NFRs in all female MDSCs. The Figure is annotated as in Figure 3. **B)** CpG methylation is low at baseline and further reduced in Old Sepsis. **C)** GCH plots confirm persistent, high-level accessibility in all conditions, suggesting these promoters regulate core cellular functions.

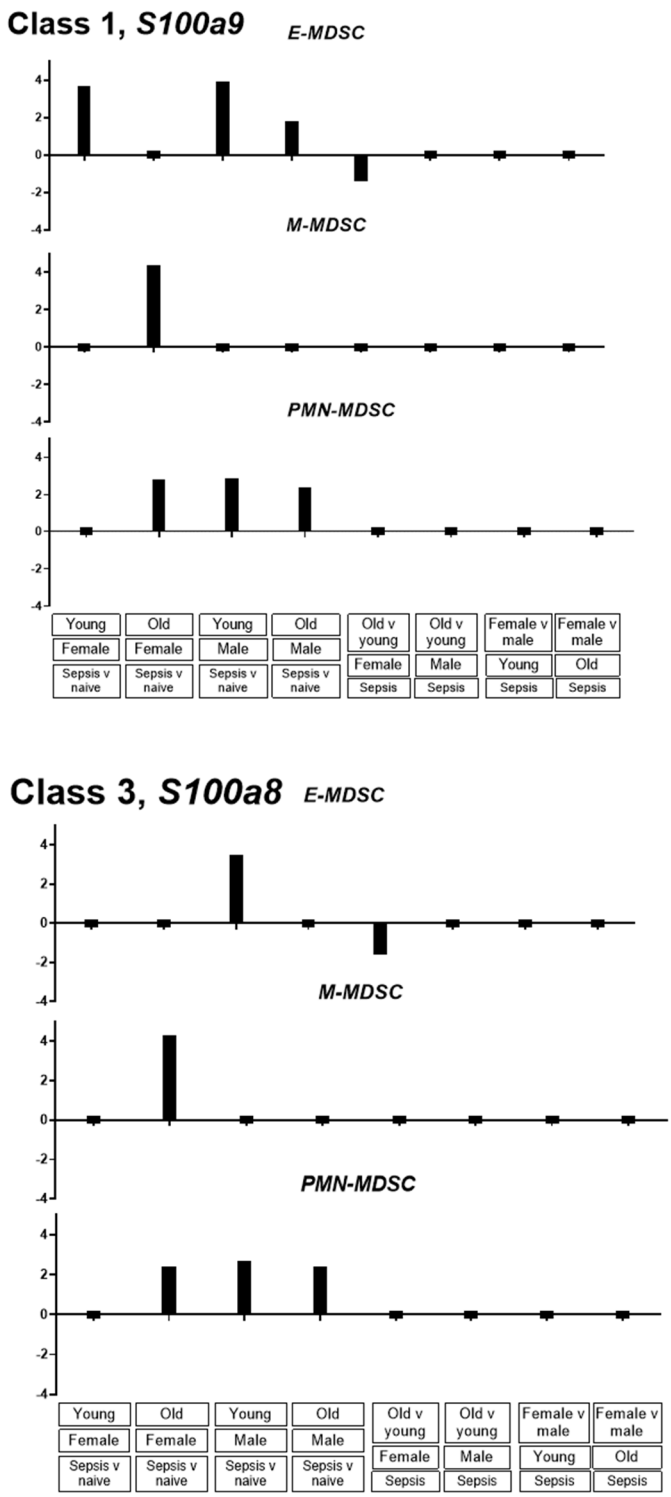

Figure 13. Class 1 and Class 3 genes show consistent sepsis-induced transcriptional activation across MDSC subsets. Bar plots $\log_2$ fold change in expression for *S100a9* (Class 1)

and *S100a8* (Class 3) across E-MDSC, M-MDSC, and PMN-MDSC populations (conditions and comparisons as labeled) derived from single-cell RNA-seq analysis of splenic $Cd11b^{+}$ $Gr1^{+}$ cells.

Class 7, *Ccl5*

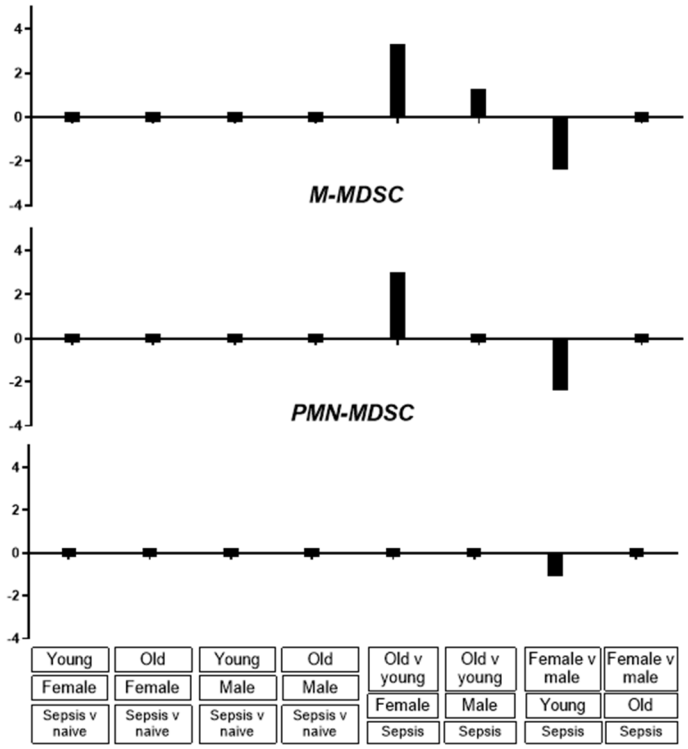

Class 8, *Nfkbiz*

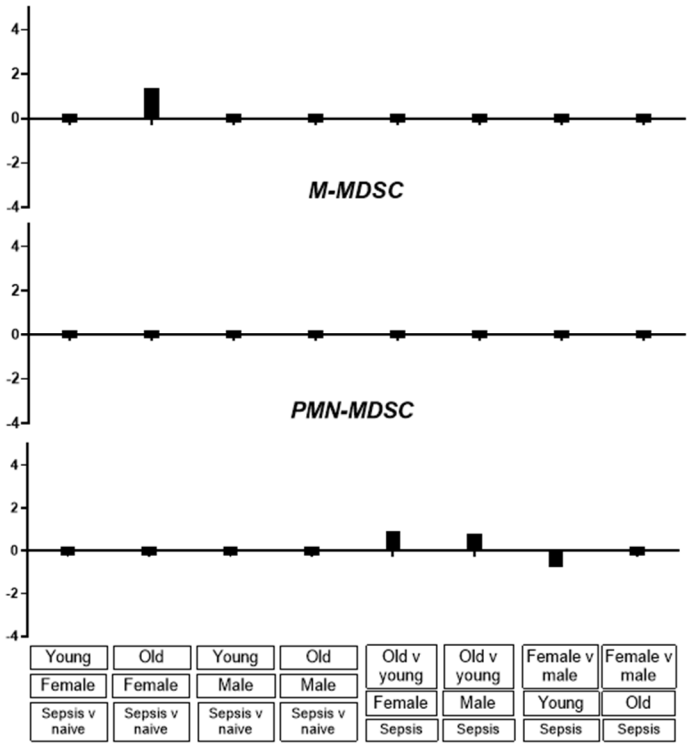

Figure 14. Expression of Class 7 and Class 8 genes across MDSC subtypes reveals repression and age-dependent silencing. Bar plots depict $\log_2$ fold change in gene expression (conditions and comparisons as labeled) for *Ccl5* (Class 7) and *Nfkbiz* (Class 8), derived from single-cell RNA-seq analysis of splenic $Cd11b^+$ $Gr1^+$ cells. Data are shown separately for early MDSCs (E-MDSC), monocytic MDSCs (M-MDSC), and polymorphonuclear MDSCs (PMN-MDSC).

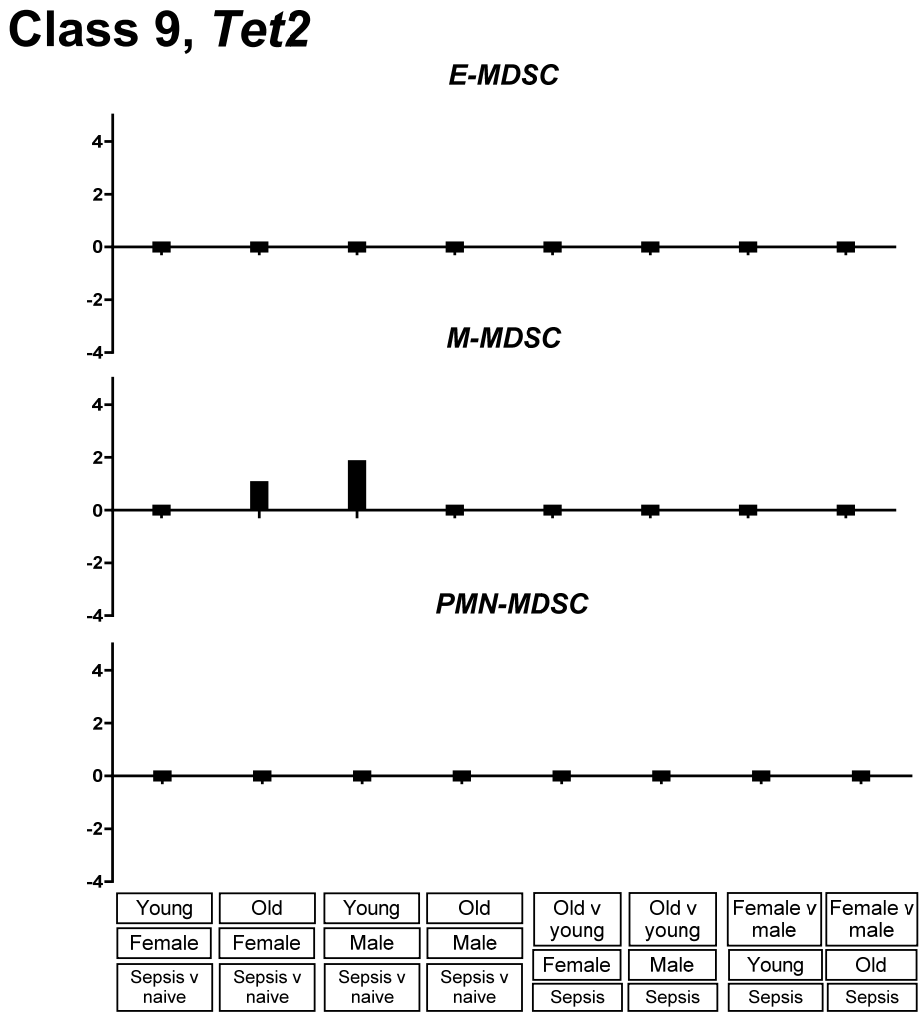

Figure 15. Expression of the Class 9 gene *Tet2* across MDSC subtypes reveals repression and age-dependent silencing. Bar plots depict $\log_2$ fold change in gene expression (conditions and comparisons as labeled) for *Tet2* (Class 9), derived from single-cell RNA-seq analysis of splenic $Cd11b^+$ $Gr1^+$ cells. Data are shown separately for early MDSCs (E-MDSC), monocytic MDSCs (M-MDSC), and polymorphonuclear MDSCs (PMN-MDSC).

Epigenetic Class	Gene Promoters
1	*S100a9*
2	*Ccl3, Cxcr2, Il1rl2, Lcn2, Lgals9, Nos2, Ptgs2, Rnase2a*
3	*Mmp8, Ros1, S100a8*
4	*Fyb*
5	*Dab2, Emp1, F7, Lyz1, Mmp19, Pmp22, Retn, Serpina1a, Vnn1, Vsig4*
6	*Ambp, Ccl5, Cd9, Cxcl3, Fabp7, Fgr, Gpnmb, Kdm6b, Lgals2, Mmp9, Saa3, Serpine1, Sparc*
7	*Car4, Ccl17, Gprc5b, Htr2a, Igkv12-44, Igkv12-46, Igkv4-69 , Il10, Mt2, Plac8, S100a10, Stab1, Tmem176a, Tmem176a, Vcan*
8	*Atf6, Cd274, Hdac3, Il4ra, Nfkbiz, Vdr*
9	*Jun, Tet2, Stat3*

Table 1: Gene Promoters Grouped by Epigenetic Class

References

1. Schepp W, Classen M. Omeprazole in the acute treatment of gastric ulcer. Scand J Gastroenterol Suppl. 1989;166:58–62; discussion 74–5. doi: 10.3109/00365528909091246. PubMed PMID: 2690333.

2. Rhee C, Dantes R, Epstein L, Murphy DJ, Seymour CW, Iwashyna TJ, Kadri SS, Angus DC, Danner RL, Fiore AE, Jernigan JA, Martin GS, Septimus E, Warren DK, Karcz A, Chan C, Menchaca JT, Wang R, Gruber S, Klompas M, Program CDCPE. Incidence and Trends of Sepsis in US Hospitals Using Clinical vs Claims Data, 2009-2014. Jama. 2017;318(13):1241–9. doi: 10.1001/jama.2017.13836. PubMed PMID: 28903154; PMCID: PMC5710396.

3. Hollenbeak CS, Henning DJ, Geeting GK, Ledeboer NA, Faruqi IA, Pierce CG, Thomas CB, O'Neal HR, Jr. Costs and Consequences of a Novel Emergency Department Sepsis Diagnostic Test: The IntelliSep Index. Crit Care Explor. 2023;5(7):e0942. Epub 20230714. doi: 10.1097/CCE.0000000000000942. PubMed PMID: 37465702; PMCID: PMC10351935.

4. Darden DB, Brakenridge SC, Efron PA, Ghita GL, Fenner BP, Kelly LS, Mohr AM, Moldawer LL, Moore FA. Biomarker Evidence of the Persistent Inflammation, Immunosuppression and Catabolism Syndrome (PICS) in Chronic Critical Illness (CCI) After Surgical Sepsis. Ann Surg. 2021;274(4):664–73. doi: 10.1097/SLA.0000000000005067. PubMed PMID: 34506322; PMCID: PMC8592255.

5. Brakenridge SC, Efron PA, Cox MC, Stortz JA, Hawkins RB, Ghita G, Gardner A, Mohr AM, Anton SD, Moldawer LL, Moore FA. Current Epidemiology of Surgical Sepsis: Discordance Between Inpatient Mortality and 1-year Outcomes. Ann Surg. 2019;270(3):502–10. doi: 10.1097/SLA.0000000000003458. PubMed PMID: 31356275; PMCID: PMC6942687.

6. Herran-Monge R, Muriel-Bombin A, Garcia-Garcia MM, Merino-Garcia PA, Martinez-Barrios M, Andaluz D, Ballesteros JC, Dominguez-Berrot AM, Moradillo-Gonzalez S, Macias S, Alvarez-Martinez B, Fernandez-Calavia MJ, Tarancon C, Villar J, Blanco J. Epidemiology and Changes in Mortality of Sepsis After the Implementation of Surviving Sepsis Campaign Guidelines. J Intensive Care Med. 2019;34(9):740–50. Epub 20170626. doi: 10.1177/0885066617711882. PubMed PMID: 28651474.

7. Polcz VE, Barrios EL, Larson SD, Efron PA, Rincon JC. Charting the course for improved outcomes in chronic critical illness: therapeutic strategies for persistent inflammation, immunosuppression, and catabolism syndrome (PICS). Br J Anaesth. 2024;133(2):260–3. Epub 20240619. doi: 10.1016/j.bja.2024.05.005. PubMed PMID: 38902117.

8. Gabrilovich DI, Bronte V, Chen SH, Colombo MP, Ochoa A, Ostrand-Rosenberg S, Schreiber H. The terminology issue for myeloid-derived suppressor cells. Cancer Res. 2007;67(1):425; author reply 6. doi: 10.1158/0008-5472.CAN-06-3037. PubMed PMID: 17210725; PMCID: PMC1941787.

9. Veglia F, Sanseviero E, Gabrilovich DI. Myeloid-derived suppressor cells in the era of increasing myeloid cell diversity. Nat Rev Immunol. 2021;21(8):485–98. Epub 20210201. doi: 10.1038/s41577-020-00490-y. PubMed PMID: 33526920; PMCID: PMC7849958.

10. Mira JC, Gentile LF, Mathias BJ, Efron PA, Brakenridge SC, Mohr AM, Moore FA, Moldawer LL. Sepsis Pathophysiology, Chronic Critical Illness, and Persistent Inflammation-Immunosuppression and Catabolism Syndrome. Crit Care Med. 2017;45(2):253–62. doi: 10.1097/CCM.0000000000002074. PubMed PMID: 27632674; PMCID: PMC5243156.

11. Uhel F, Azzaoui I, Gregoire M, Pangault C, Dulong J, Tadie JM, Gacouin A, Camus C, Cynober L, Fest T, Le Tulzo Y, Roussel M, Tarte K. Early Expansion of Circulating Granulocytic Myeloid-derived Suppressor Cells Predicts Development of Nosocomial Infections in Patients with Sepsis. Am J Respir Crit Care Med. 2017;196(3):315–27. doi: 10.1164/rccm.201606-1143OC. PubMed PMID: 28146645.

12. Mathias B, Delmas AL, Ozrazgat-Baslanti T, Vanzant EL, Szpila BE, Mohr AM, Moore FA, Brakenridge SC, Brumback BA, Moldawer LL, Efron PA, the Sepsis CIRCI. Human Myeloid-derived Suppressor Cells are Associated With Chronic Immune Suppression After Severe Sepsis/Septic Shock. Ann Surg. 2017;265(4):827–34. doi: 10.1097/SLA.0000000000001783. PubMed PMID: 27163951; PMCID: PMC5102824.

13. Barrios EL, Leary JR, Darden DB, Rincon JC, Willis M, Polcz VE, Gillies GS, Munley JA, Dirain ML, Ungaro R, Nacionales DC, Gauthier ML, Larson SD, Morel L, Loftus TJ, Mohr AM, Maile R, Kladde MP, Mathews CE, Brusko MA, Brusko TM, Moldawer LL, Bacher R, Efron PA. The post-septic peripheral myeloid compartment reveals unexpected diversity in myeloid-derived suppressor cells. Front Immunol. 2024;15:1355405. Epub 20240424. doi: 10.3389/fimmu.2024.1355405. PubMed PMID: 38720891; PMCID: PMC11076668.

14. Darden DB, Bacher R, Brusko MA, Knight P, Hawkins RB, Cox MC, Dirain ML, Ungaro R, Nacionales DC, Rincon JC, Gauthier ML, Kladde M, Bihorac A, Brusko TM, Moore FA, Brakenridge SC, Mohr AM, Moldawer LL, Efron PA. Single-Cell RNA-seq of Human Myeloid-Derived Suppressor Cells in Late Sepsis Reveals Multiple Subsets With Unique Transcriptional Responses: A Pilot Study. Shock. 2021;55(5):587–95. doi: 10.1097/SHK.0000000000001671. PubMed PMID: 33021571; PMCID: PMC8019679.

15. Hollen MK, Stortz JA, Darden D, Dirain ML, Nacionales DC, Hawkins RB, Cox MC, Lopez MC, Rincon JC, Ungaro R, Wang Z, Wu Q, Brumback B, Gauthier ML, Kladde M, Leeuwenburgh C, Segal M, Bihorac A, Brakenridge S, Moore FA, Baker HV, Mohr AM, Moldawer LL, Efron PA. Myeloid-derived suppressor cell function and epigenetic expression evolves over time after surgical sepsis. Crit Care. 2019;23(1):355. Epub 20191113. doi: 10.1186/s13054-019-2628-x. PubMed PMID: 31722736; PMCID: PMC6854728.

16. Efron PA, Brakenridge SC, Mohr AM, Barrios EL, Polcz VE, Anton S, Ozrazgat-Baslanti T, Bihorac A, Guirgis F, Loftus TJ, Rosenthal M, Leeuwenburgh C, Mankowski R, Moldawer LL, Moore FA. The persistent inflammation, immunosuppression, and catabolism syndrome 10 years later. J Trauma Acute Care Surg. 2023;95(5):790–9. Epub 20230808. doi: 10.1097/TA.0000000000004087. PubMed PMID: 37561664; PMCID: PMC10615691.

17. Efron PA, Darden DB, Li EC, Munley J, Kelly L, Fenner B, Nacionales DC, Ungaro RF, Dirain ML, Rincon J, Mankowski RT, Leeuwenburgh C, Moore FA, Brakenridge SC, Foster TC, Laitano O, Casadesus G, Moldawer LL, Mohr AM, Thomas RM. Sex differences associate with late microbiome alterations after murine surgical sepsis. J Trauma Acute Care Surg. 2022;93(2):137–46. Epub 20220324. doi: 10.1097/TA.0000000000003599. PubMed PMID: 35324554; PMCID: PMC9323556.

18. Rani A, Barter J, Kumar A, Stortz JA, Hollen M, Nacionales D, Moldawer LL, Efron PA, Foster TC. Influence of age and sex on microRNA response and recovery in the hippocampus following sepsis. Aging (Albany NY). 2022;14(2):728–46. Epub 20220130. doi: 10.18632/aging.203868. PubMed PMID: 35094981; PMCID: PMC8833110.

19. Mankowski RT, Thomas RM, Darden DB, Gharaibeh RZ, Hawkins RB, Cox MC, Apple C, Nacionales DC, Ungaro RF, Dirain ML, Moore FA, Leeuwenburgh C, Brakenridge SC, Clanton TL, Laitano O, Moldawer LL, Mohr AM, Efron PA. Septic Stability? Gut Microbiota in Young Adult Mice Maintains Overall Stability After Sepsis Compared to Old Adult Mice. Shock. 2021;55(4):519–25. doi: 10.1097/SHK.0000000000001648. PubMed PMID: 32826817; PMCID: PMC7895866.

20. Mankowski RT, Anton SD, Ghita GL, Brumback B, Cox MC, Mohr AM, Leeuwenburgh C, Moldawer LL, Efron PA, Brakenridge SC, Moore FA. Older Sepsis Survivors Suffer Persistent Disability Burden and Poor Long-Term Survival. J Am Geriatr Soc. 2020;68(9):1962–9. Epub 20200415. doi: 10.1111/jgs.16435. PubMed PMID: 32294254; PMCID: PMC7654284.

21. Stortz JA, Hollen MK, Nacionales DC, Horiguchi H, Ungaro R, Dirain ML, Wang Z, Wu Q, Wu KK, Kumar A, Foster TC, Stewart BD, Ross JA, Segal M, Bihorac A, Brakenridge S, Moore FA, Wohlgemuth SE, Leeuwenburgh C, Mohr AM, Moldawer LL, Efron PA. Old Mice Demonstrate Organ Dysfunction as well as Prolonged Inflammation, Immunosuppression, and Weight Loss in a Modified Surgical Sepsis Model. Crit Care Med. 2019;47(11):e919–e29. doi: 10.1097/CCM.0000000000003926. PubMed PMID: 31389840; PMCID: PMC6848973.

22. Barter J, Kumar A, Stortz JA, Hollen M, Nacionales D, Efron PA, Moldawer LL, Foster TC. Age and Sex Influence the Hippocampal Response and Recovery Following Sepsis. Mol

Neurobiol. 2019;56(12):8557–72. Epub 20190705. doi: 10.1007/s12035-019-01681-y. PubMed PMID: 31278440; PMCID: PMC6834928.

23. Brakenridge SC, Efron PA, Stortz JA, Ozrazgat-Baslanti T, Ghita G, Wang Z, Bihorac A, Mohr AM, Brumback BA, Moldawer LL, Moore FA. The impact of age on the innate immune response and outcomes after severe sepsis/septic shock in trauma and surgical intensive care unit patients. J Trauma Acute Care Surg. 2018;85(2):247–55. doi: 10.1097/TA.0000000000001921. PubMed PMID: 29613958; PMCID: PMC6081244.

24. Raymond SL, Lopez MC, Baker HV, Larson SD, Efron PA, Sweeney TE, Khatri P, Moldawer LL, Wynn JL. Unique transcriptomic response to sepsis is observed among patients of different age groups. PLoS One. 2017;12(9):e0184159. Epub 20170908. doi: 10.1371/journal.pone.0184159. PubMed PMID: 28886074; PMCID: PMC5590890.

25. Nacionales DC, Szpila B, Ungaro R, Lopez MC, Zhang J, Gentile LF, Cuenca AL, Vanzant E, Mathias B, Jyot J, Westerveld D, Bihorac A, Joseph A, Mohr A, Duckworth LV, Moore FA, Baker HV, Leeuwenburgh C, Moldawer LL, Brakenridge S, Efron PA. A Detailed Characterization of the Dysfunctional Immunity and Abnormal Myelopoiesis Induced by Severe Shock and Trauma in the Aged. J Immunol. 2015;195(5):2396–407. Epub 20150805. doi: 10.4049/jimmunol.1500984. PubMed PMID: 26246141; PMCID: PMC4546902.

26. Gjerstorff MF. Epigenetic targeting of myeloid-derived suppressor cells: time to move into infectious diseases? Front Immunol. 2023;14:1247715. Epub 20230823. doi: 10.3389/fimmu.2023.1247715. PubMed PMID: 37680643; PMCID: PMC10482232.

27. Zhou M, Nabilsi NH, Wang A, Gauthier M-PL, Murray KO, Azari H, Owens WS, Newman JRB, Pardo-Palacios FJ, Conesa A, Riva A, Clanton TL, Reynolds BA, Concannon P, Brant JO, Bacher R, Kladde MP. Flap-enabled next-generation capture (FENGC): precision

targeted single-molecule profiling of epigenetic heterogeneity, chromatin dynamics, and genetic variation. bioRxiv. 2022–11–09. doi: 10.1101/2022.11.08.515732.

28. Nacionales DC, Gentile LF, Vanzant E, Lopez MC, Cuenca A, Cuenca AG, Ungaro R, Li Y, Baslanti TO, Bihorac A, Moore FA, Baker HV, Leeuwenburgh C, Moldawer LL, Efron PA. Aged mice are unable to mount an effective myeloid response to sepsis. J Immunol. 2014;192(2):612–22. Epub 20131213. doi: 10.4049/jimmunol.1302109. PubMed PMID: 24337739; PMCID: PMC3884685.

29. Bible LE, Pasupuleti LV, Gore AV, Sifri ZC, Kannan KB, Mohr AM. Chronic restraint stress after injury and shock is associated with persistent anemia despite prolonged elevation in erythropoietin levels. J Trauma Acute Care Surg. 2015;79(1):91–6; discussion 6–7. doi: 10.1097/TA.0000000000000686. PubMed PMID: 26091320; PMCID: PMC4902106.

30. Hao Y, Stuart T, Kowalski MH, Choudhary S, Hoffman P, Hartman A, Srivastava A, Molla G, Madad S, Fernandez-Granda C, Satija R. Dictionary learning for integrative, multimodal and scalable single-cell analysis. Nat Biotechnol. 2024;42(2):293–304. Epub 20230525. doi: 10.1038/s41587-023-01767-y. PubMed PMID: 37231261; PMCID: PMC10928517.

31. Korsunsky I, Millard N, Fan J, Slowikowski K, Zhang F, Wei K, Baglaenko Y, Brenner M, Loh PR, Raychaudhuri S. Fast, sensitive and accurate integration of single-cell data with Harmony. Nat Methods. 2019;16(12):1289–96. Epub 20191118. doi: 10.1038/s41592-019-0619-0. PubMed PMID: 31740819; PMCID: PMC6884693.

32. JR S, MA H, T S, Y K, CE P, NH N, RP D, R P, K I, S H, MP K, J B. High Fractional Occupancy of a Tandem Maf Recognition Element and Its Role in Long-Range β-Globin Gene

Regulation - PubMed. Molecular and cellular biology. 10/26/2015;36(2). doi: 10.1128/MCB.00723-15.

33. P K, ML G, CE P, RP D, K K, H B, E M, A R, MP K, R B. Methylscaper: an R/Shiny app for joint visualization of DNA methylation and nucleosome occupancy in single-molecule and single-cell data - PubMed. Bioinformatics (Oxford, England). 12/11/2021;37(24). doi: 10.1093/bioinformatics/btab438.

34. von Wulffen M, Luehrmann V, Robeck S, Russo A, Fischer-Riepe L, van den Bosch M, van Lent P, Loser K, Gabrilovich DI, Hermann S, Roth J, Vogl T. S100A8/A9-alarmin promotes local myeloid-derived suppressor cell activation restricting severe autoimmune arthritis. Cell Rep. 2023;42(8):113006. Epub 20230822. doi: 10.1016/j.celrep.2023.113006. PubMed PMID: 37610870.

35. Davison LM, Alberto AA, Dand HA, Keller EJ, Patt M, Khan A, Dvorina N, White A, Sakurai N, Liegl LN, Vogl T, Jorgensen TN. S100a9 Protects Male Lupus-Prone NZBWF1 Mice From Disease Development. Front Immunol. 2021;12:681503. Epub 20210617. doi: 10.3389/fimmu.2021.681503. PubMed PMID: 34220829; PMCID: PMC8248531.

36. Groth C, Hu X, Weber R, Fleming V, Altevogt P, Utikal J, Umansky V. Immunosuppression mediated by myeloid-derived suppressor cells (MDSCs) during tumour progression. Br J Cancer. 2019;120(1):16–25. Epub 20181109. doi: 10.1038/s41416-018-0333-1. PubMed PMID: 30413826; PMCID: PMC6325125.

37. Santibanez JF. Myeloid-Derived Suppressor Cells: Implications in Cancer Immunology and Immunotherapy. Front Biosci (Landmark Ed). 2025;30(3):25203. doi: 10.31083/FBL25203. PubMed PMID: 40152373.

38. Wang S, Zhao X, Wu S, Cui D, Xu Z. Myeloid-derived suppressor cells: key immunosuppressive regulators and therapeutic targets in hematological malignancies. Biomark Res. 2023;11(1):34. Epub 20230329. doi: 10.1186/s40364-023-00475-8. PubMed PMID: 36978204; PMCID: PMC10049909.

39. Ibrahim AA, Fujimura T, Uno T, Terada T, Hirano KI, Hosokawa H, Ohta A, Miyata T, Ando K, Yahata T. Plasminogen activator inhibitor-1 promotes immune evasion in tumors by facilitating the expression of programmed cell death-ligand 1. Front Immunol. 2024;15:1365894. Epub 20240508. doi: 10.3389/fimmu.2024.1365894. PubMed PMID: 38779680; PMCID: PMC11109370.

40. Brune JE, Chang MY, Altemeier WA, Frevert CW. Type I Interferon Signaling Increases Versican Expression and Synthesis in Lung Stromal Cells During Influenza Infection. J Histochem Cytochem. 2021;69(11):691–709. Epub 20211019. doi: 10.1369/00221554211054447. PubMed PMID: 34666527; PMCID: PMC8554580.

41. Chang MY, Tanino Y, Vidova V, Kinsella MG, Chan CK, Johnson PY, Wight TN, Frevert CW. A rapid increase in macrophage-derived versican and hyaluronan in infectious lung disease. Matrix Biol. 2014;34:1–12. Epub 20140126. doi: 10.1016/j.matbio.2014.01.011. PubMed PMID: 24472738; PMCID: PMC4019684.

42. Yaseen MM, Abuharfeil NM, Darmani H, Daoud A. Mechanisms of immune suppression by myeloid-derived suppressor cells: the role of interleukin-10 as a key immunoregulatory cytokine. Open Biol. 2020;10(9):200111. Epub 20200916. doi: 10.1098/rsob.200111. PubMed PMID: 32931721; PMCID: PMC7536076.

43. Wang JC, Sun L. PD-1/PD-L1, MDSC Pathways, and Checkpoint Inhibitor Therapy in Ph(-) Myeloproliferative Neoplasm: A Review. Int J Mol Sci. 2022;23(10). Epub 20220523. doi: 10.3390/ijms23105837. PubMed PMID: 35628647; PMCID: PMC9143160.

44. Jayakumar A, Bothwell ALM. Functional Diversity of Myeloid-Derived Suppressor Cells: The Multitasking Hydra of Cancer. J Immunol. 2019;203(5):1095–103. doi: 10.4049/jimmunol.1900500. PubMed PMID: 31427398; PMCID: PMC6703177.

45. Jauch-Speer SL, Herrera-Rivero M, Ludwig N, Veras De Carvalho BC, Martens L, Wolf J, Imam Chasan A, Witten A, Markus B, Schieffer B, Vogl T, Rossaint J, Stoll M, Roth J, Fehler O. C/EBPdelta-induced epigenetic changes control the dynamic gene transcription of S100a8 and S100a9. Elife. 2022;11. Epub 20220511. doi: 10.7554/eLife.75594. PubMed PMID: 35543413; PMCID: PMC9122501.

46. Pappritz K, Voss I, El-Shafeey M, Van Linthout S. Sex differences in age-related cardiac and splenic S100A9 and NLRP3 expression. J Leukoc Biol. 2025. Epub 20250315. doi: 10.1093/jleuko/qiaf031. PubMed PMID: 40086818.

47. Stadtmann A, Zarbock A. CXCR2: From Bench to Bedside. Front Immunol. 2012;3:263. Epub 20120824. doi: 10.3389/fimmu.2012.00263. PubMed PMID: 22936934; PMCID: PMC3426767.

48. Li S, Feng J, Wu F, Cai J, Zhang X, Wang H, Fetahu IS, Iwanicki I, Ma D, Hu T, Liu H, Wang B, Shi G, Tan L, Shi YG. TET2 promotes anti-tumor immunity by governing G-MDSCs and CD8(+) T-cell numbers. EMBO Rep. 2020;21(10):e49425. Epub 20200914. doi: 10.15252/embr.201949425. PubMed PMID: 32929842; PMCID: PMC7534639.

49. Cai Z, Kotzin JJ, Ramdas B, Chen S, Nelanuthala S, Palam LR, Pandey R, Mali RS, Liu Y, Kelley MR, Sandusky G, Mohseni M, Williams A, Henao-Mejia J, Kapur R. Inhibition of

Inflammatory Signaling in Tet2 Mutant Preleukemic Cells Mitigates Stress-Induced Abnormalities and Clonal Hematopoiesis. Cell Stem Cell. 2018;23(6):833–49 e5. doi: 10.1016/j.stem.2018.10.013. PubMed PMID: 30526882; PMCID: PMC6317370.

50. Barrios EL, Rincon JC, Willis M, Polcz VE, Leary JR, Darden DB, Balch JA, Larson SD, Loftus TJ, Mohr AM, Wallet S, Brusko MA, Balzano-Nogueira L, Cai G, Sharma A, Upchurch GR, Jr., Kladde MP, Mathews CE, Maile R, Moldawer LL, Bacher R, Efron PA. Transcriptomic Differences in Peripheral Monocyte Populations in Septic Patients Based on Outcome. Shock. 2024;62(2):208–16. Epub 20240502. doi: 10.1097/SHK.0000000000002379. PubMed PMID: 38713581.

51. Balch JA, Chen UI, Liesenfeld O, Starostik P, Loftus TJ, Efron PA, Brakenridge SC, Sweeney TE, Moldawer LL. Defining critical illness using immunological endotypes in patients with and without sepsis: a cohort study. Crit Care. 2023;27(1):292. Epub 20230720. doi: 10.1186/s13054-023-04571-x. PubMed PMID: 37474944; PMCID: PMC10360294.

52. Sherwood ER, Burelbach KR, McBride MA, Stothers CL, Owen AM, Hernandez A, Patil NK, Williams DL, Bohannon JK. Innate Immune Memory and the Host Response to Infection. J Immunol. 2022;208(4):785–92. doi: 10.4049/jimmunol.2101058. PubMed PMID: 35115374; PMCID: PMC8982914.

53. Rincon JC, Wang D, Polcz VE, Barrios EL, Dirain ML, Ungaro RF, Nacionales DC, Zeumer-Spataro L, Xiao F, Efron PA, Moldawer LL, Cai G, Larson SD. Innate immune training in the neonatal response to sepsis. Molecular medicine. 2025;31(1):159. Epub 20250430. doi: 10.1186/s10020-025-01179-5. PubMed PMID: 40307728; PMCID: PMC12042443.